ผลเฉลยเชิงวิเคราะห์ของหน่วยแรงทีทั่วไปในตัวกลางไพอิโซอิเลคทริคภายใต้เงื่อนไขขอบเขตที่ผิวรอยร้าวแบบต่างๆ

นายวิเชธ ชาน พิช

วิทยานิพนธ์นี้เป็นส่วนหนึ่งของการศึกษาตามหลักสูตรปริญญาวิศวกรรมศาสตรมหาบัณฑิต
สาขาวิชาวิศวกรรมโยธา ภาควิชาวิศวกรรมโยธา
คณะวิศวกรรมศาสตร์ จุฬาลงกรณ์มหาวิทยาลัย
ปีการศึกษา 2558

ANALYTICAL SOLUTIONS OF GENERALIZED T-STRESS IN LINEAR PIEZOELECTRIC MEDIA UNDER VARIOUS CRACK-FACE CONDITIONS

Mr. Vichet Chan Pich

A Thesis Submitted in Partial Fulfillment of the Requirements
for the Degree of Master of Engineering Program in Civil Engineering
Department of Civil Engineering
Faculty of Engineering
Chulalongkorn University
Academic Year 2015

Thesis Title	ANALYTICAL SOLUTIONS OF GENERALIZED T-STRESS IN LINEAR PIEZOELECTRIC MEDIA UNDER VARIOUS CRACK-FACE CONDITIONS
By	Mr. Vichet Chan Pich
Field of Study	Civil Engineering
Thesis Advisor	Associate Professor Jaroon Rungamornrat, Ph.D.
Thesis Co-Advisor	Weeraporn Phongtinnaboot, Ph.D.

Accepted by the Faculty of Engineering, Chulalongkorn University in Partial Fulfillment of the Requirements for the Master's Degree

.....Dean of the Faculty of Engineering
(Associate Professor Supot Teachavorasinskun, D.Eng.)

THESIS COMMITTEE

.....Chairman
(Professor Teerapong Senjuntichai, Ph.D.)

.....Thesis Advisor
(Associate Professor Jaroon Rungamornrat, Ph.D.)

.....Thesis Co-Advisor
(Weeraporn Phongtinnaboot, Ph.D.)

.....Examiner
(Associate Professor Akhrawat Lenwari, Ph.D.)

.....External Examiner
(Yasothorn Sapsathiarn, Ph.D.)

วิเชธ ชาน พิช : ผลเฉลยเชิงวิเคราะห์ของหน่วยแรงทีทั่วไปในตัวกลางไพอิโซอิเลคทริคภายใต้เงื่อนไขขอบเขตที่ผิวรอยร้าวแบบต่างๆ (ANALYTICAL SOLUTIONS OF GENERALIZED T-STRESS IN LINEAR PIEZOELECTRIC MEDIA UNDER VARIOUS CRACK-FACE CONDITIONS) อ.ที่ปรึกษาวิทยานิพนธ์หลัก: รศ. ดร. จรูญ รุ่งอมรรัตน์, อ. ที่ปรึกษาวิทยานิพนธ์ร่วม: ดร. วีรพร พงศ์ติณบุตร, 68 หน้า.

วิทยานิพนธ์ฉบับนี้นำเสนอผลเฉลยแบบเปิดของหน่วยแรงทีทั่วไปของรอยร้าววงกลมในตัวกลางทรานเวอร์สลีย์ไอโซทรอปิกไพอิโซอิเล็กทริกไร้ขอบเขตภายใต้เงื่อนไขที่ผิวรอยร้าวแบบต่างๆกัน อาทิเช่น เงื่อนไขแบบซึมผ่านได้ แบบซึมผ่านไม่ได้ แบบซึมผ่านได้บางส่วน และแบบสอดคล้องเชิงพลังงาน ผลเฉลยในกรณีของแรงกระทำระยะไกลและแรงกระทำที่ผิวรอยร้าวทั้งแบบเชิงกลและเชิงไฟฟ้าถูกพัฒนาขึ้นสำหรับเงื่อนไขที่ผิวรอยร้าวทั้งสี่ประเภท ส่วนผลเฉลยของรอยร้าวที่รับแรงกระทำคู่แบบจุดที่ผิวรอยร้าวถูกพัฒนาขึ้นสำหรับเงื่อนไขที่ผิวรอยร้าวแบบซึมผ่านได้และแบบซึมผ่านไม่ได้เท่านั้น การพัฒนาผลเฉลยใช้สนามหน่วยแรงทั่วไปที่พบในงานวิจัยในอดีตร่วมกับสูตรที่ได้จากการกระจายสนามบริเวณใกล้ขอบรอยร้าว ค่าอนุพันธ์และลิมิตที่เกี่ยวข้องหาได้โดยอาศัยกระบวนการมาตรฐานและผลเฉลยสุดท้ายของหน่วยแรงทีทั่วไปเกี่ยวข้องเฉพาะฟังก์ชันพื้นฐานเท่านั้น นอกจากนี้ฟังก์ชันของกรีนสำหรับหน่วยแรงทีทั่วไปที่ได้ถูกนำมาใช้ในการพัฒนาสูตรเชิงปริพันธ์สำหรับใช้คำนวณค่าหน่วยแรงทีทั่วไปของรอยร้าวแบบซึมผ่านได้และซึมผ่านไม่ได้ภายใต้แรงกระทำที่ผิวรอยร้าวแบบทั่วไป คุณลักษณะเชิงวิเคราะห์และกึ่งเชิงวิเคราะห์ของผลเฉลยที่ได้มีบทบาทสำคัญในการศึกษาอิทธิพลของพารามิเตอร์ต่างๆที่มีผลต่อค่าหน่วยแรงทีทั่วไปบริเวณขอบรอยร้าว อาทิเช่น เงื่อนไขที่ผิวรอยร้าว แรงเชิงกลและเชิงไฟฟ้าระยะไกล แรงกระทำที่ผิวรอยร้าว และคุณสมบัติวัสดุ เป็นต้น สุดท้ายมีการนำเสนอผลที่ได้จากการศึกษาพร้อมข้อสรุปที่สำคัญ

ภาควิชา วิศวกรรมโยธา ลายมือชื่อนิสิต .....

สาขาวิชา วิศวกรรมโยธา ลายมือชื่อ อ.ที่ปรึกษาหลัก .....

ปีการศึกษา 2558 ลายมือชื่อ อ.ที่ปรึกษาร่วม .....

5770529221 : MAJOR CIVIL ENGINEERING
KEYWORDS: CRACK-FACE CONDITIONS / GENERALIZED T-STRESS / GREEN'S FUNCTION / PENNY-SHAPED CRACK / PIEZOELECTRIC MEDIUM

VICHET CHAN PICH: ANALYTICAL SOLUTIONS OF GENERALIZED T-STRESS IN LINEAR PIEZOELECTRIC MEDIA UNDER VARIOUS CRACK-FACE CONDITIONS. ADVISOR: ASSOC. PROF. JAROON RUNGAMORNRAT, Ph.D., CO-ADVISOR: WEERAPORN PHONGTINNABOOT, Ph.D., 68 pp.

This thesis presents the closed-form solution of the generalized T-stress components of a penny-shaped crack in a transversely isotropic, linear piezoelectric, infinite medium under different crack-face conditions including electrically permeable, impermeable, semi-permeable and energetically consistent conditions. The solution for the case of uniform remote and crack-face mechanical/electrical loadings are derived for all four crack-face conditions whereas that for a crack under a pair of self-equilibrated, crack-face concentrated loads is obtained for permeable and impermeable cases. In the derivation, existing analytical solutions of the generalized stress field are employed together with an explicit expression resulting from the asymptotic expansion of the near-front field. All involved differentiations and limits are carried out in a careful manner following standard procedures and the final solution of the generalized T-stress components involves only elementary functions. In addition, the established Green’s function for the generalized T-stress is utilized to form an integral formula capable of computing the generalized T-stress for impermeable and permeable cracks under general crack-face loading. The analytical/semi-analytical feature of the derived solutions play a key role in the investigation of the influence of various parameters such as the crack-face conditions, electrical/mechanical far field, and the crack-face loading on the value of the generalized T-stress components along the crack front. A selected set of results is reported and significant and useful findings are concluded.

Department:	Civil Engineering	Student's Signature .....
Field of Study:	Civil Engineering	Advisor's Signature .....
Academic Year:	2015	Co-Advisor's Signature .....

ACKNOWLEDGEMENTS

First of all, I would like to express my sincere thanks to my advisor, Assoc. Prof. Dr. Jaroon Rungamornrat, who always gives me support, meaningful comments and good advises for the investigations of the entire thesis. Secondly, I would like to thank to my co-advisor, Dr. Weeraporn Phongtinnaboot, for providing me both comments and requirement journals to complete my thesis. Thirdly, I would like to gratefully acknowledge financial support from JICA AUN/SEED-Net scholarship and acceptation from Department of Civil Engineering, Chulalongkorn University that provide me an opportunity to pursue master degree. Lastly, I would like to express my thanks to my family, my friends and everyone who always give me courage till completion of this thesis.

CONTENTS

Page

Page

LIST OF FIGURES

LIST OF SYMBOLES

D_i Electrical induction vector

d_3 General surface charge acting to crack surface

d_3^0 Uniform electrical charge acting to crack surface

d^∞ Uniform remote electrical induction ($\{d_1^\infty, d_2^\infty, d_3^\infty\}$)

E_{ijkm} Elastic constants

E_i Electric field

E_{iJKl} Generalized moduli

e_{mij} Piezoelectric constants

$f_{,\mathrm{i}}$ Partial derivative of function f with respect to coordinate x_i

r Radial coordinate of polar coordinate system (r,θ)

$\overline{r}$ Radial coordinate of polar coordinate system $(\overline{r},\overline{\theta})$

T_Q Generalized T-stress components

T_{iJ} All components of generalized T-stress

T_Q^{GP} Generalized T-stress Green's function under a pair of unit normal point forces

T_Q^{GE} Generalized T-stress Green's function under a pair of unit point charges

T_Q^∞ Generalized T-stress components due to uniform remote triaxial generalized stress σ_{iJ}^∞

T_Q^0 Generalized T-stress components due to uniform part of the general applied traction t_3 and general electrical charge d_3

T_Q^1 Generalized T-stress components due to remaining non-uniform part of general applied traction t_3 and general electrical charge d_3

t_J Components of generalized traction

t_3 General normal traction acting to crack surface

t_3^0 Uniform normal traction acting to crack surface

u_i Components of displacement

u_J Components of generalized displacement

$\boldsymbol{x}_c$ Origin of local coordinate system $\{\boldsymbol{x}_c; \overline{x}_1, \overline{x}_2, \overline{x}_3\}$

σ_{ij} Component of stress

σ_{iJ} Components of generalized stress

$\boldsymbol{\sigma}^{\infty}$ Uniform remote triaxial stress ($\{\sigma_{11}^{\infty}, \sigma_{22}^{\infty}, \sigma_{33}^{\infty}\}$)

$\bar{\sigma}_{iJ}$ Local components of generalized stress

$\bar{\sigma}_{iJ}^{K}$ Function independent of radial coordinate contained in singular term

$\bar{\sigma}_{iJ}^{T}$ Function independent of radial coordinate contained in first non-singular term

$\bar{\sigma}_{iJ}^{(m)}$ Function independent of radial coordinate contained in other non-singular terms vanishing along crack front

$\bar{\sigma}_{iJ}^{\infty}$ Local components of uniform remote triaxial generalized stresses

$\bar{\sigma}_{iJ}^{GP}$ Local components of generalized stress Green's function under a pair of unit normal point forces

$\bar{\sigma}_{iJ}^{GE}$ Local components of generalized stress Green's function under a pair of unit point charges

σ_i Mechanical traction normal to the crack surface

$\Delta\sigma_i$ Jump of crack-face mechanical normal traction

Δu_j Jump of crack-face displacement

Δt_4 Jump of crack-face surface electric charge

ε_{im} Dielectric permittivity

$\bar{\varepsilon}_{ij}$ Strain tensor

ϕ Electric potential

τ_i Mechanical tractions tangent to the crack surface

κ_c Dielectric permittivity of medium inside crack gap

Chapter 1

INTRODUCTION

This chapter firstly illustrates the significance of piezoelectric materials, their recent applications in various fields, motivation of the present study, and then provides the brief background and review of relevant literatures in modeling and analysis of fractures in piezoelectric media. Next, the key objectives and scope of work are clearly defined as well as the methodology and research procedure. Finally, the expected outcome and contribution of the present work is addressed.

1.1 Significance and Motivation

Piezoelectric materials have been found possessing unique properties which enable to transform mechanical energy into electrical energy or vice versa. Such strong electro-mechanical coupling effect is widely known as the piezoelectric effect (including both the direct and converse piezoelectric effects). Owing to these abilities, piezoelectric materials have been utilized in many applications in various disciplines such as aerospace and automotive industries, acoustic field, engineering and medical applications. Additionally, piezoelectric materials have also been found as constituting materials of the key components of many recent advanced devices and structures including piezoelectric power supplies, the electro-mechanical sensors and actuators, the sonar transducers, and smart and self-adaptive structures. However, one obvious drawback of this particular class of materials is their brittle characteristics associated with possessing relatively low fracture toughness and high sensitivity to flaw inducing. In addition, these piezoelectric-based devices often operate under various circumstances that may be prone to fracture-induced damages and failures. For instance, vibration detector sensors are designed to capture the earthquake motion; loud speakers receive electric signals and convert them into mechanical vibrations which create sound waves to produce the desirable acoustic; and the piezoelectric floors, which have been trailed in some stations in Japan, generate the electricity from walking pedestrian for automatic ticket gates and electronic display systems. As a direct consequence of their key properties and

applications, cracks/defects are unavoidably found inside piezoelectric bodies under usages. Therefore, when subjected to mechanical, electrical, or electrical-mechanical excitations, these piezoelectric components and devices can encounter the degradations, damages, and ultimate failure as a result of preexisting or loaded induced cracks/defects. Understanding of fundamental fracture characteristics and fracture-induced failure mechanism is obviously essential and required in the design of piezoelectric components and devices to maintain their safety and integrity.

Mathematical modeling and simulations, based mainly on the classical theory of linear piezoelectricity, have been vastly applied in literature and found effective and efficient for the generalized stress analysis of piezoelectric cracked bodies. The generalized stress field in the neighborhood of the crack boundary (including the mechanical stress and the electric induction), predicted from the linear theory, dominates characteristics of the cracked medium and has been found essential as the basic information for simulating cracks initiations and advances. Most of existing studies in the context of linear piezoelectric fracture mechanics focused mainly on the dominant singular terms in the near-front expansion of the generalized stress field and, the corresponding parameters such as the electric and stress intensity factors and generalized strain energy release rate have been often used in the growth criteria. Numerous researches have been carried out to demonstrate the significance of these crack-front parameters, for instance, the crack formation, the subsequent crack propagation, and the damage and failure (Zhou et al., 2013). Nevertheless, existing experimental and theoretical evidences have also indicated the significant contribution of the non-singular term of the near-tip generalized stress, known as the generalized T-stress, and the necessity to integrate such information in the fracture modeling. Within the context of elastic media, the T-stress is viewed as the boundary effect by following the study of Shahani and Tabatabaei (2009). In addition, the T-stress also found to strongly influence the shape and size of plastic zones, the crack-front stress constraint and tri-axiality, and the directional stability of advancing crack (Larsson & Carlsson, 1973; Cotterell & Rice, 1980; Du & Hancock, 1991; Matvienko & Pochinkov, 2013; Matvienko, 2014). The experimental study by Ayatollahi and Safari (2003) also confirmed that the rotation of the isochromatic

fringes pattern is also affected by the sign of the T-stress. In addition, the shielding or anti-shielding characteristics of the plastic-zone size and shape at the crack front is dependent on the negative and positive values of the T-stress (Zhou et al., 2011). For piezoelectric media, several investigators also concluded that the generalized T-stress is essential quantities affecting the crack-kinking behavior and the plastic zone shapes (Zhu & Yang, 1999; Hao & Biao, 2004; Li & Lee, 2004a,b; Viola et al., 2008) . These past evidences confirmed the significance of the generalized T-stress and ignorance of such crucial fracture information can, in fact, lead to the inaccurate prediction of fracture responses. As an essential step to integrate the information of the generalized T-stress in the fracture modeling, analytical and computational procedures must be properly adopted to accurately and efficiently determine those quantities along the crack front. From limited advances of researches in this particular area as supported by a careful survey of literature in the following section, the development of a solution methodology to extract the fracture data of the generalized T-stress still requires further investigations and its merit to the community of fracture mechanics should be remarkable.

1.2 Literature Review

This section mainly reviews and summarizes relevant researches concerning the historical development and current advances of techniques for deriving both the T-stress in linear elastic cracks media and the generalized T-stress in linear piezoelectric crack bodies. Although, the proposed research directly involve the calculation of the generalized T-stress, the review of existing studies for the linear elastic case is considered a pre-requisite and the close connection to the current work should offer certain insights both in terms of the significant contribution of the generalized T-stress and the solution techniques. Finally, the treatment of various electrical crack-face conditions in previous studies is discussed at the end of this section.

Regarding to linear elastic cracks media, non-singular (or finite) part of stress in the near-front expansion of the stress field have been well investigated and a vast amount of researches have been published regarding to the calculations of the T-

stresses and the study of their effect on the crack-tip stress field and fracture process. For instance, Sladek and Sladek (1997) developed a boundary integral equation method to compute the T-stress for interface cracks of a two-dimensional, semi-infinite, dissimilar materials subjected to a point force at the crack tip. Fett (1997) also derived T-stress green's functions due to a pair of normal concentrated forces and then used the obtained result to develop a boundary collocation technique to determine the T-stress of an edged-crack embedded in a rectangular plate made of a linear isotropic elastic material and subjected to general normal traction. Later, Fett (1998) extended his previous research to investigate linearly elastic rectangular plate and circular disks containing various crack configurations such as edged cracks and centered cracks and subjected to both tensile and bending loads. Yang and Ravi (1999) proposed the stress-difference method together with an iterative dual boundary integral equation method along with the tip-node displacement jump to compute the T-stress at a crack tip for thermo-elastic crack problems. Later, Chen (2000) applied the complex-potential-function theory to develop the solution of the T-stress for four types of cracks including a line crack, a symmetric airfoil crack, circular-arc crack, and a symmetric lip crack in a two-dimensional, linear elastic, infinite plate. Zhao et al. (2001) applied the domain integral and interaction integral technique to obtain numerical solution for the T-stresses of a quarter-circular crack and a tunnel-corner crack in an elastic square plate under remote tension. Their results indicated the good agreement with experimental observations, for instance, the discrepancies of the fatigue crack growth rate between CN (corner notch) and CT (compact tension) test specimens, and the crack tunneling in CN specimens under pre-dominantly sustained load. Fett (2001) utilized the same technique as that by Fett (1997) to investigate a circular disk containing an internal crack under different types of boundary conditions such as pure displacement boundary conditions, pure traction boundary conditions and mix boundary conditions. Fett (2002) extended his previous work to treat different crack configurations in both single and double edge cracked circular disks. Wang (2002) used the finite element technique together with the weight-function approach to compute the T-stress for several test specimens, for instance, CCP (a centered crack

plate), SECP (a single edged crack plate) and DECP (a double edged crack plate). The applied crack-face normal traction with either uniform, linear, parabolic, or cubic variation was investigated. Fett and Rizzi (2006) made use of the finite element procedure and the weight-function approach to determine the T-stresses for CT (a compact tension crack), DCC (a double cantilever crack), and ECB (an edge cracked bar) under self-equilibrated general normal traction near the crack tip. Also, Fett et al. (2006) employed Green's function technique to obtain the T-stress of a forked crack and a kinked crack in a plated made of an isotropic, linearly elastic material and subjected to in-plane shear and normal tractions. Recently, the T-stress of an edged crack embedded in a plate which is made of two different isotropic linearly elastic materials was studied by Zhou et al. (2013). A symplectric expansion method was employed in this particular work, and it was found efficient for treating complex boundary conditions.

While various researches concerning the two-dimensional problems have been carried out, simplified assumptions used in the modeling can lead to an inaccurate prediction and the loss of certain essential information and, as a consequence, the full three-dimensional analysis have been continuously proposed. Various existing methods for calculating the T-stress of cracks in three-dimensional media are briefly summarized and discussed below. Wang (2003) generalized the work of Wang (2002) to treat a three-dimensional crack problem by utilizing the finite element method together with the interaction integral formula to obtain the T-stresses of a surface-breaking, semi-elliptical crack in an isotropic, linearly elastic finite thick plate under bending and tensile loadings. Later, Wang and Bell (2004) further extended his previous research to treat other types of loading with different spatial variations (e.g., uniform, linear, parabolic, and cubic distribution). Wang (2004) applied the potential-theory-based method and the Hankel integral transformation to determine an exact solution for the T-stress of a penny-shaped crack contained in an isotropic, linearly elastic, infinite body under applied remote tension and bending loads. Qu and Wang (2006) determined the T-stress of a corner-quarter-elliptical crack in an isotropic, linearly elastic, thick plate via the finite element method and the interaction integral formula. Both tensile and bending loads applied at both ends

of the plate were considered in their study. Kirilyuk and Levchuk (2007) presented the T-stress solution of a flat-elliptical crack contained in an isotopic, linearly elastic, infinite body under the remote axial tension and bending loads. This research is the extension of the work of Wang (2004) by utilizing a special set of harmonic functions instead of the Hankel integrals. Zhou and Li (2007) and Zhou et al. (2011) also presented the analytical solution of the T-stress under both mode-I and mode-II conditions for the crack-inclusion interaction by using Eshelby equivalent inclusion method. Most recently, Rungamornrat and Pinitpanich (2016) utilized the existing stress field from Fabrikant (1989) together with conventional differentiations and limit procedure to derive Green's functions for the T-stress of a circular crack under a pair of opposite, normal point forces. A superposition method along with a numerical quadrature was then adopted to construct an integral formula capable of computing the T-stress components for a circular crack in a three-dimensional, transversely isotropic, linear elastic medium subjected to general applied normal traction on the crack surface.

While significant advances and progress of the modeling and analysis for the T-stress have been well recognized in the literature for various crack geometries and loading conditions, work concerning the generalized T-stress in piezoelectric cracked bodies is still limited. This may result from not only the complexity of electro-mechanical coupling effect but also the lack of recognition of the generalized T-stress and its contribution. The brief overview of relevant literatures concerning the determination of the generalized T-stress solution is presented and discussed in a chronological order as follows. Zhu and Yang (1999) confirmed the contribution of the generalized T-stress on the crack-kinking behavior for a straight crack embedded in a piezoelectric, two-dimensional body under prescribed mechanical loading conditions. In their study, the continuous dislocation theory and a boundary integral equation method were employed. Hao and Biao (2004) derived the exact solution of the generalized T-stresses of an impermeable straight crack embedded in a transversely isotropic, linear piezoelectric whole space under applied mechanical and electrical loading conditions. In their study, the principle of superposition along the Plemelji formulation was utilized. Results from this investigation also indicated

that the value of the generalized T-stress depends mainly on the elastic, piezoelectric constants, and dielectric permittivity. In the same year, Li and Lee (2004a) applied Fourier transform to formulate a pair of dual integral equations and then derived the analytical solution of a semi-permeable Griffith crack oriented normal to the poling direction and subjected to uniform electro-mechanical loading conditions. Later, Zhong and Li (2008) reported the closed-form solution of the generalized T-stress for a semi-permeable Griffith crack in a two-dimensional, transversely isotropic, linear piezoelectric solid under the remote uniform mechanical tension, electrical induction and magnetic effect. In their analytical study, the Fourier integral transform along with the standard procedure was applied to solve the dual integral equation to obtain the complete solution. Liu et al. (2012) studied an elliptical hole embedded in a two-dimensional, transversely isotropic, linear piezoelectric, infinite body subjected to the uniform pressure at the surface of the hole and the remote electro-mechanical loads. The complete analytical solution of both mechanical and electrical fields for the electrical permeable boundary condition was obtained by applying the complex variable function approach. They also pointed out that the behavior of the electric induction and stress in the vicinity of the crack front depends strongly on the value of the non-singular term. Most recently, Subsathaphol (2013) developed a numerical procedure based upon the weakly singular, boundary integral equation technique and standard Galerkin procedure to extract the generalized T-stress components of an impermeable isolated cracks contained in three-dimensional, anisotropic, piezoelectric, infinite media under general mechanical/electrical loading conditions.

Another important issue effecting the calculation of the generalized T-stress components of cracks in piezoelectric media is the model used to simulate the crack-face conditions. Various models have been proposed to simulate such crack-face conditions and the key difference among those models stems directly from the assumption of the dielectric permittivity of a medium filled within crack cavity. Suitability of all existing models is still questionable, highly problem dependent, and, therefore, requires further investigations. The electrical impermeable and electrical permeable crack-face conditions are two idealized models that have been widely

employed in the linear piezoelectric fracture modeling due to their mathematical simplicity. The permeable model, proposed by Parton (1976), assumes the continuity of a normal component of the electrical induction and the electrical potential across the geometrically identical crack surfaces. This is opposite to the impermeable model where the electric induction normal to surface of the crack is fully prescribed whereas the crack-face electrical potential is unknown a priori and discontinuous. It should be remarked that these two crack-face models could provide an inaccurate prediction of solution due to the ignorance of the influence of permittivity. In order to improve the modeling, Hao and Shen (1994) developed a semi-permeable electrical boundary condition which includes the effect of the dielectric permittivity of the medium within the crack cavity on the continuity of the electric field across the crack gap. In this point of view, the electrical impermeable and electrical permeable conditions are simply two extreme cases of the semi-permeable crack-face condition. Later, McMeeking (2004) found that the total energy and the crack-tip energy release rates of a Griffith crack resulting from the use of the semi-permeable condition are not consistent. To overcome the energy inconsistency, Landis (2004) further modified the original semi-permeable model to obtain an energetically consistent model by integrating the traction normal to the crack face.

From the comprehensive review of all involved literatures, most the existing solutions for the T-stress of cracks in elastic bodies have been well-established in the context of both two-dimensional and three-dimensional boundary value problems. However, the analytical and numerical solutions of the generalized T-stress have been very limited and restricted mostly to very simple settings. In addition, the integration of more suitable electrical crack-face conditions such as those described by energetically consistent and semi-permeable models in the determination of the generalized T-stress components and the study of their effects on that essential fracture data have not been well recognized. These existing gaps of knowledge directly motivate the proposed research.

1.3 Research Objective

This research aims mainly to derive analytical and semi-analytical solutions of the generalized T-stress components for a penny-shaped (or circular) crack in piezoelectric media under various crack-face conditions and to preliminary explore the effect of crack-face conditions and crack-face loading on the generalized T-stress components along the crack boundary.

1.4 Scope of Work

The present work is carried out within following context:

(1) A cracked medium is three-dimensional and occupies the whole space.

(2) A piezoelectric material is assumed linear, homogeneous, and transversely isotropic with the poling direction and the axis of material symmetry normal to the crack surface.

(3) A body is free of the body force and distributed electric charge.

(4) A penny-shaped crack under various loading and crack-face conditions is considered.

  (4.1) For an impermeable crack, remote uniform mechanical/electrical loads, a pair of opposite normal concentrated forces acting on the crack surface, a pair of opposite concentrated charges acting on the crack surface, and arbitrarily distributed, crack-face normal traction and crack-face surface charge are considered.

  (4.2) For a permeable crack, remote uniform mechanical/electrical loads, a pair of opposite normal concentrated forces acting on the crack surface, and arbitrarily distributed, crack-face normal traction are considered.

  (4.3) For a semi-permeable crack, uniform remote mechanical/electrical loads and uniformly distributed, crack-face normal traction are considered.

  (4.4) For an energetically consistent crack, uniform remote mechanical/ electrical loads are considered.

1.5 Research Methodology

The proposed research mainly involves the development of both analytical and semi-analytical solutions of the generalized T-stress for various cases as indicated above. Available complete solutions of the generalized stress field for a circular crack subjected to fundamental loading conditions and various types of crack-face conditions are employed as the basis for the derivation of the generalized T-stress and the essential Green's functions. To accomplish all proposed tasks, following fundamental theories, methodology and research procedure are employed.

(1) Basis field equations including conservation law, kinematics, and constitutive relationship follow a classical theory of linear piezoelectricity.

(2) The crack-face condition is simulated by four mathematical models including electrically permeable, electrically impermeable, electrically semi-permeable, and energetically consistent conditions.

(3) Basic equations, crack-face conditions, and prescribed loading conditions are integrated to form a set of boundary value problems.

(4) Closed-form solutions of the generalized stress field for certain fundamental cases, such as cracks under a pair of opposite normal concentrated forces (impermeable and permeable cases), a pair of self-equilibrated charges (impermeable case), and uniform remote mechanical/electrical loads (all crack-face conditions), are collected from existing literature.

(5) A formula involving differentiations and limits is developed based on the near-front expansion of the generalized stress field for extracting the generalized T-stress. This formula together with standard differentiations and a proper limiting process is then employed to compute the generalized T-stress Green's function and the generalized T-stress components for all fundamental cases.

(6) A method of superposition is applied together with the developed generalized T-stress Green's function to establish the integral formula for the generalized T-stress components for both impermeable and permeable

penny-shaped cracks under arbitrarily distributed, crack-face surface charge and normal traction.

(7) An efficient quadrature is employed to compute all involved singular integrals in the integral formula for general crack-face loading conditions.

(8) The influence of crack-face loading conditions and crack-face conditions on the generalized T-stress components on the crack boundary is preliminary investigated.

1.6 Expected Outcome and Contribution

The present research offers (i) the closed-form expression of the generalized T-stress components for a circular crack under uniform remote mechanical/electrical loads and various crack-face conditions, (ii) the integral formula of the generalized T-stress for an impermeable circular crack under arbitrarily distributed, crack-face, normal traction and surface charge, (iii) the integral formula of the generalized T-stress components for a permeable circular crack under arbitrarily distributed normal traction, and (iv) fundamental understanding of the effect of various parameters such as the crack-face and loading conditions on the generalized T-stress components on the crack boundary. The derived solution can be also employed as the reliable benchmark solution in the verification procedure of computational techniques developed for modeling more general crack problems.

Chapter 2

PROBLEM FORMULATION

This chapter begins with describing basic field equations essential for formulating boundary value problems of linear piezoelectricity and, also, providing the definition of all involved parameters. Following sections present the clear description of the crack-face conditions considered in the present study, the near-front generalized stress field and essential formula for extracting the generalized T-stress, the superposition method employed to formulate the integral formula of the generalized T-stress components, and, finally, existing solutions of the generalized stress field for certain fundamental cases.

2.1 Basic Field Equations

Basic equations for a medium with zero body forces and body electric charges are adopted from the classical theory of linear piezoelectricity. The laws of conservation are expressed explicitly by

$$\begin{aligned} \sigma_{ij,i} &= 0 \\ D_{i,i} &= 0 \end{aligned} \tag{2-1}$$

where σ_{ij} denotes components of a stress tensor; D_i denotes components of an electrical induction vector; the comma notation $f_{,\mathrm{i}}$ represents a partial derivative of any function f with respect to a Cartesian coordinate x_i; and standard indicial notations apply. Here and in what follows, a standard indicial notation applies; specifically, lower-case subscripts range from 1 to 3 and the repeated lower-case index indicates the summation over its range. Components of the stress tensor and electric induction vector are linearly related to the electric field with its components denoted by E_i and the strain tensor with its components denoted by $\overline{\varepsilon}_{ij}$ via a set of fully coupled linear algebraic equations

$$\begin{aligned} \sigma_{ij} &= E_{ijkm}\overline{\varepsilon}_{km} - e_{mij}E_m \\ D_i &= e_{ikm}\overline{\varepsilon}_{km} + \varepsilon_{im}E_m \end{aligned} \tag{2-2}$$

where E_{ijkm} denotes the elastic constants; e_{mij} denotes the piezoelectric constants; and ε_{im} denotes the dielectric permittivity. The electric field E_i and the strain tensor $\bar{\varepsilon}_{ij}$ are given in terms of components of the displacement vector, denoted by u_i, and the electric potential, denoted by ϕ, via the following linearized kinematics

$$\begin{aligned} \bar{\varepsilon}_{ij} &= \frac{1}{2}\left(u_{i,j} + u_{j,i}\right) \\ E_i &= -\phi_{,i} \end{aligned} \tag{2-3}$$

Components of the mechanical traction, denoted by t_i, and the surface electric charge, denoted by D, at any point on the smooth boundary can be computed in terms of the stress field and the electric induction vector by

$$\begin{aligned} t_i &= \sigma_{ij} n_j \\ D &= D_j n_j \end{aligned} \tag{2-4}$$

where n_j denote components of an outward unit normal vector to the smooth surface. All field equations (2-1)-(2-3) can also be expressed in a more concise form (suggested by (Rungamornrat & Mear, 2008)) as follows:

$$\sigma_{iJ,i} = 0 \tag{2-5}$$

$$\sigma_{iJ} = E_{iJKm} u_{K,m} \tag{2-6}$$

where upper-case index ranges from 1 to 4 and the repeated upper-case index indicates the summation over its range; σ_{iJ} is termed the generalized stress which contains components of the stress tensor σ_{ij} and components of the electrical induction vector $\sigma_{i4} \equiv D_i$; u_J is termed the generalized displacement which contains components of the displacement u_j and the electrical potential $u_4 \equiv \phi$; and E_{iJKl} is termed the generalized moduli which contains elastic moduli E_{ijkl}, piezoelectric constants $E_{ij4l} \equiv E_{l4ij} \equiv e_{lij}$, and dielectric permittivity $E_{i44l} \equiv E_{l44i} \equiv -\varepsilon_{il}$. Consistent with this new notation, the generalized traction, denoted by t_J and computed from $t_J \equiv \sigma_{iJ} n_i$, contains the mechanical traction $t_j = \sigma_{ij} n_i$ and the surface electric charge $t_4 \equiv \sigma_{i4} n_i = D$. It can be remarked that the generalized

moduli E_{iJKl} defined above possesses the following symmetric property $E_{iJKl} = E_{lJKi}$ provided that E_{l4ji} is selected to be identical to E_{ij4l}.

2.2 Crack-face Conditions

On the surface of the crack, the condition on the crack-face data such as the generalized displacement on the upper crack surface (S_c^+) and the lower crack surface (S_c^+), denoted by u_J^+ and u_J^-, respectively, and the generalized traction on both the upper and lower crack surfaces, denoted by t_J^+ and t_J^-, respectively, must be properly prescribed. In the current investigation, four types of crack-face models including electrically permeable, impermeable, semi-permeable, and energetically consistent crack-face conditions are treated (see details in Rungamornrat et al. (2015)).

For an impermeable crack model, the crack-face generalized traction t_J^+ and t_J^- are fully prescribed whereas the crack-face generalized displacements u_J^+ and u_J^- are unknown a priori. For a permeable crack model, the mechanical crack-face tractions t_j^+ and t_j^- are fully prescribed and the jump in the crack-face electrical potential and the sum of the crack-face surface electrical charge vanishes (i.e., $\Delta u_4 \equiv u_4^+ - u_4^- = 0$ and $\Sigma t_4 \equiv t_4^+ + t_4^- = 0$) whereas the sum of the crack-face generalized displacement $\Sigma u_J \equiv u_J^+ + u_J^-$, the jump in the crack-face displacement $\Delta u_j \equiv u_j^+ - u_j^-$, and the jump in the crack-face surface electrical charge $\Delta t_4 \equiv t_4^+ - t_4^-$ are unknown a priori. For a semi-permeable crack model, the crack-face generalized displacement u_J^+ and u_J^-, and the jump in the crack-face surface electric charge Δt_4 are unknown a priori whereas the mechanical crack-face tractions t_j^+ and t_j^- are fully known, the sum of the crack-face surface electrical charge vanishes (i.e., $\Sigma t_4 = 0$), and the following nonlinear relationship is satisfied

$$t_4^+ \Delta u_i n_i^+ = -\kappa_c \Delta u_4 \tag{2-7}$$

where κ_c denotes the dielectric permittivity of a medium filled within the crack cavity. Finally, for an energetically consistent crack model, the crack-face generalized displacement u_J^+ and u_J^-, the jump in the crack-face surface electrical charge Δt_4, and the jump in the mechanical crack-face normal traction, denoted by

$\Delta\sigma_i \equiv \sigma_i^+ - \sigma_i^-$ where $\sigma_i^+ = t_j^+ n_j n_i$ and $\sigma_i^- = t_j^- n_j n_i$, are unknown a priori whereas the mechanical crack-face shear tractions, denoted by $\tau_i^+ = t_i^+ - \sigma_i^+$ and $\tau_i^- = t_i^- - \sigma_i^-$ are fully known, the sum of the crack-face surface electrical charge and the sum of the mechanical crack-face shear traction vanish (i.e., $\Sigma t_4 = 0$ and $\Sigma\sigma_i \equiv \sigma_i^+ + \sigma_i^- = 0$), and the following two nonlinear relations are satisfied

$$\begin{aligned} & t_4^+ \Delta u_i n_i^+ = -\kappa_c \Delta u_4 \\ & \sigma_j^+ = (1/2)\kappa_c n_j^+ \left(\Delta u_4\right)^2 / \left(\Delta u_i n_i^+\right)^2 \end{aligned} \tag{2-8}$$

It is emphasized that the superscripts "+" and "−" are used only to designate quantities on the upper crack surface and the lower crack surface, respectively.

2.3 Description of Problem

Consider a three-dimensional body occupying the whole space and containing a circular (or penny-shaped) crack with the radius *a* as shown in Figure 2.1. For convenience, the reference Cartesian coordinate system $\{\mathbf{0}; x_1, x_2, x_3\}$ and the associated cylindrical reference coordinate system $\{\mathbf{0}; r, \theta, z\}$ are introduced such that an origin $\mathbf{0}$ is located at the crack center, the x_3-axis directs upward, and the remaining axes follow the right-hand rule. A material constituting the body is assumed to be homogeneous, transversely isotropic, and linear piezoelectric. All involved material constants are fully prescribed whereas the axis of material symmetry and poling direction are assumed to direct normal to the crack surface.

Besides the basic field equations (2-1)-(2-3), the prescribed crack-face boundary conditions have been found strongly affecting responses of the piezoelectric cracked medium. Thus, the proper understanding of the role of the crack-face condition on the fracture data along the crack boundary such as the generalized intensity factors and generalized T-stress is essential and requires the full investigation. In the present study, all four models of crack-face boundary conditions indicated above are considered and the different types of mechanical/electrical loading conditions are considered as follows.

For a circular crack under the impermeable condition, six following loading cases are considered: (i) a pair of opposite, normal concentrated forces acting to the crack

surface (see Figure 2-2), (ii) a pair of opposite, concentrated electrical charge acting to the crack surface (see Figure 2.3), (iii) a self-equilibrated, crack-face, uniform normal traction t_3^0 and a self-equilibrated, crack-face, uniform surface charge d_3^0 (see Figure 2-4(a-b)), (iv) uniform remote triaxial stress $\{\sigma_{11}^{\infty}, \sigma_{22}^{\infty}, \sigma_{33}^{\infty}\}$ and a uniform remote electrical induction $\{d_1^{\infty}, d_2^{\infty}, d_3^{\infty}\}$ (see Figure 2-5), (v) general, self-equilibrated, crack-face normal traction t_3 (see Figure 2-6(a)), and (vi) general, self-equilibrated, crack-face surface electrical charge d_3 (see Figure 2-6(b)).

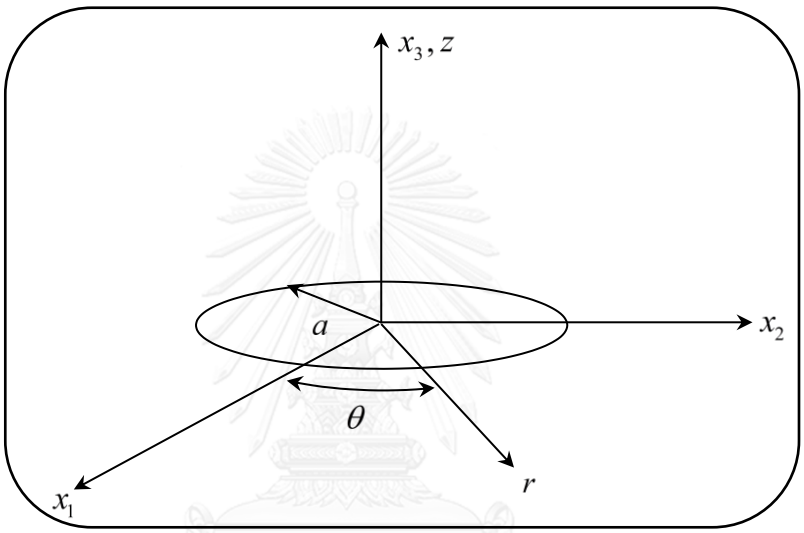

Figure 2-1: Schematic of circular crack with radius a contained in transversely isotropic, linear piezoelectric, infinite medium

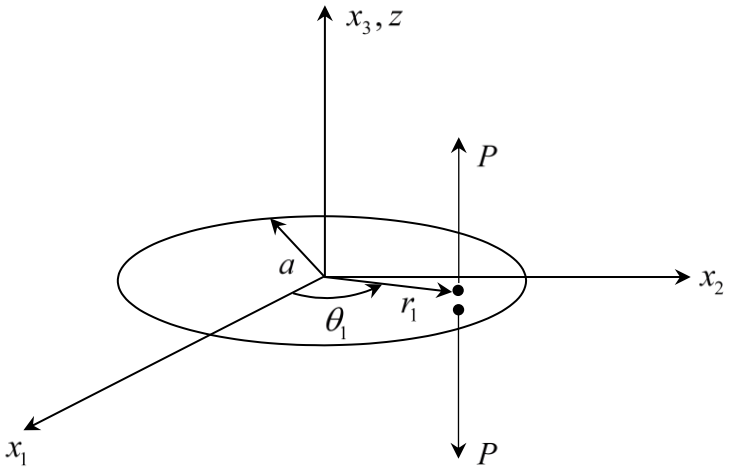

Figure 2-2: Schematic of circular crack under pair of opposite normal concentrated forces acting to crack surface

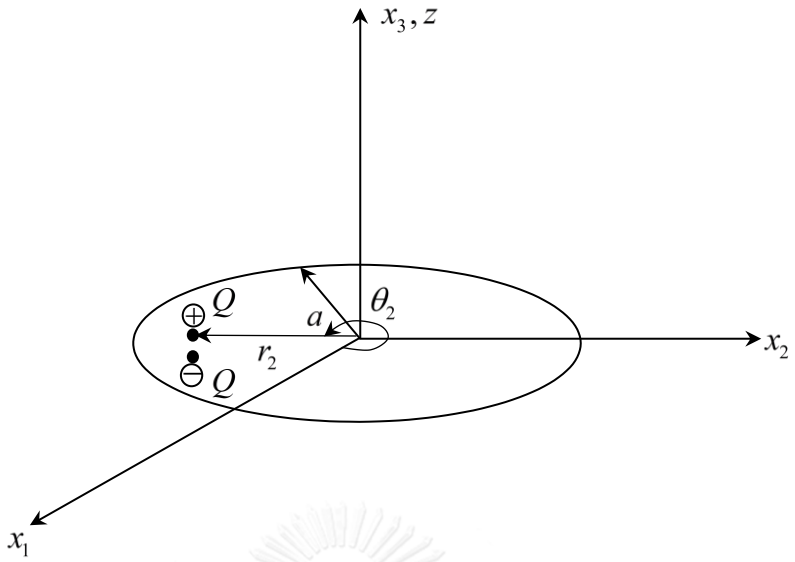

Figure 2-3: Schematic of circular crack under pair of opposite, concentrated electrical charge acting to crack surface

For a permeable circular crack, four loading cases are considered: (i) a pair of opposite, normal concentrated forces acting to the crack surface (see Figure 2-2), (ii) self-equilibrated, crack-face, uniform normal traction t_3^0 (see Figure 2-4(a)), (iii) uniform remote triaxial stress $\{\sigma_{11}^{\infty}, \sigma_{22}^{\infty}, \sigma_{33}^{\infty}\}$ and a uniform remote electrical induction $\{d_1^{\infty}, d_2^{\infty}, d_3^{\infty}\}$ (see Figure 2-5), and (iv) general, self-equilibrated, crack-face normal traction t_3 (see Figure 2-6(a)).

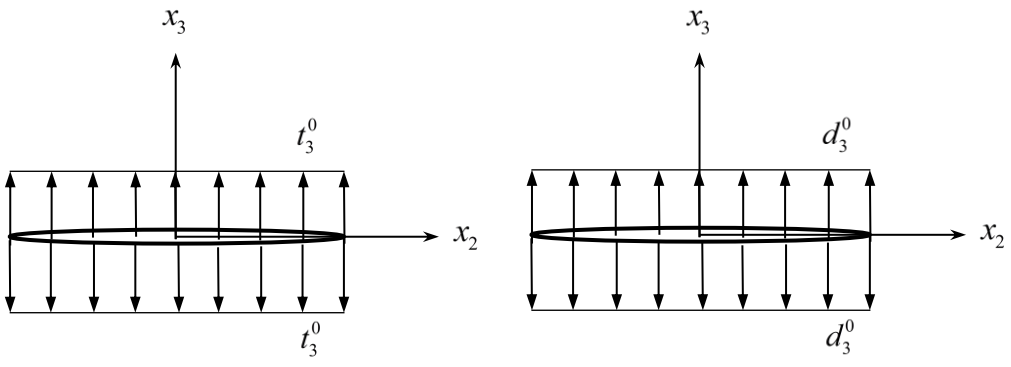

(a) (b)

Figure 2-4: Schematic of circular crack under (a) self-equilibrated, crack-face, uniform normal traction t_3^0 and (b) self-equilibrated, crack-face, uniform surface charge d_3^0

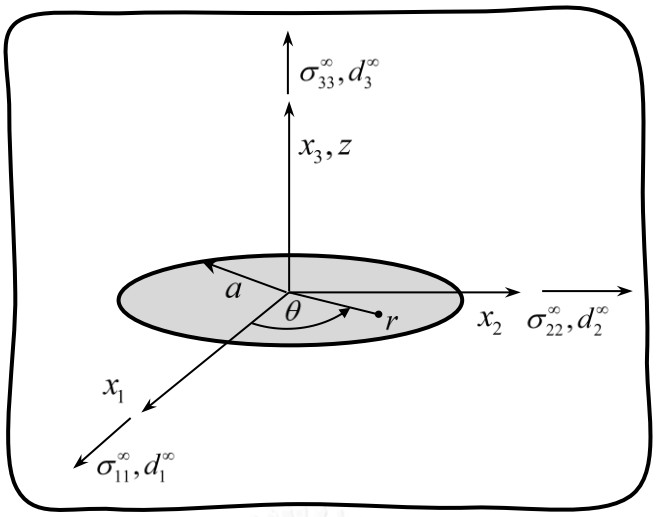

Figure 2-5: Schematic of circular crack under uniform remote triaxial stress $\{\sigma_{11}^{\infty}, \sigma_{22}^{\infty}, \sigma_{33}^{\infty}\}$ and uniform remote electrical induction $\{d_1^{\infty}, d_2^{\infty}, d_3^{\infty}\}$

For a semi-permeable penny shaped crack, two following loading cases are considered: (i) self-equilibrated, uniform normal traction t_3^0 (see Figure 2-4(a)) and (ii) a uniform remote triaxial stress $\{\sigma_{11}^{\infty}, \sigma_{22}^{\infty}, \sigma_{33}^{\infty}\}$ and a uniform remote electrical induction $\{d_1^{\infty}, d_2^{\infty}, d_3^{\infty}\}$ (see Figure 2-5). Finally, for an energetically consistent circular crack, only the constant remote triaxial stress $\{\sigma_{11}^{\infty}, \sigma_{22}^{\infty}, \sigma_{33}^{\infty}\}$ and a uniform remote electrical induction $\{d_1^{\infty}, d_2^{\infty}, d_3^{\infty}\}$ (see Figure 2-5) are considered.

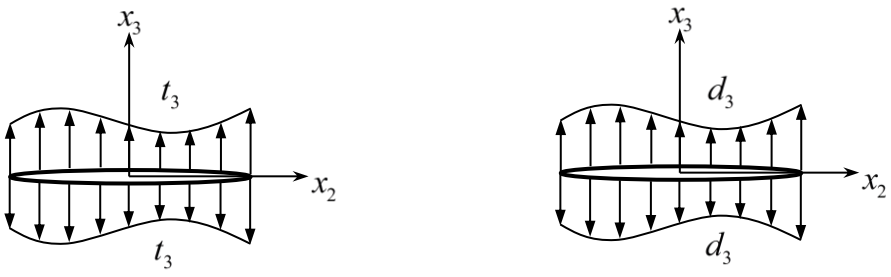

(a) (b)

Figure 2-6: Schematic of circular crack under (a) general, self-equilibrated, crack-face, normal traction and (b) general, self-equilibrated, crack-face, surface charge

2.4 Near-front Generalized Stress Field

By following an analogy as that employed by Williams (1957), the local generalized stress field in a region containing the point $\boldsymbol{x}_c$ on the crack front can be expressed as

$$\bar{\sigma}_{iJ}(\boldsymbol{x}_c;\bar{r},\bar{\theta}) = \frac{1}{\sqrt{\bar{r}}}\bar{\sigma}_{iJ}^{K}(\boldsymbol{x}_c;\theta) + \bar{\sigma}_{iJ}^{T}(\boldsymbol{x}_c;\theta) + \sum_{m=1}^{\infty}\bar{r}^{m/2}\bar{\sigma}_{iJ}^{(m)}(\boldsymbol{x}_c;\theta) \tag{2-9}$$

where the "bar" is used to designate quantities referring to the local reference coordinate system $\{\boldsymbol{x}_c;\bar{x}_1,\bar{x}_2,\bar{x}_3\}$ with the origin at $\boldsymbol{x}_c$ and the corresponding orthonormal basis $\{\bar{\boldsymbol{e}}_1,\bar{\boldsymbol{e}}_2,\bar{\boldsymbol{e}}_3\}$ such that $\bar{x}_1-\bar{x}_3$ is a tangent plane to the crack surface at $\boldsymbol{x}_c$ whereas the $\bar{x}_1-\bar{x}_2$ plane is normal to the crack front at $\boldsymbol{x}_c$ as shown in Figure 2.6; $(\bar{r},\bar{\theta})$ denotes the polar coordinates of a point in the $\bar{x}_1-\bar{x}_2$ plane; $\bar{\sigma}_{iJ}(\boldsymbol{x}_c;\bar{r},\bar{\theta})$ denotes the generalized stress at any point in the $\bar{x}_1-\bar{x}_2$ plane in the neighborhood of the point $\boldsymbol{x}_c$; $\bar{\sigma}_{iJ}^{K}$, $\bar{\sigma}_{iJ}^{T}$, and $\bar{\sigma}_{iJ}^{(m)}$ are functions independent of the radial coordinate $\bar{r}$. This asymptotic expansion of the near-front field is expressed in the same form as that appearing in Rungamornrat and Pinitpanich (2016). Regarding to the near-front expansion (2-9), it is evident that the first term represents the dominant part of the field which is singular of order $1/\sqrt{r}$ at the point $\boldsymbol{x}_c$; the second term represent the constant field that is independent of the radial coordinate $\bar{r}$, and the third term represents the non-singular part that vanishes identically at the point $\boldsymbol{x}_c$ along the crack front.

Now, let us define the components $T_{iJ}=T_{iJ}(\boldsymbol{x}_c)$ referring to the local reference coordinate system $\{\boldsymbol{x}_c;\bar{x}_1,\bar{x}_2,\bar{x}_3\}$ such that

$$T_{iJ}(\boldsymbol{x}_c) = \bar{\sigma}_{iJ}^{T}(\boldsymbol{x}_c;\bar{\theta}=0) \tag{2-10}$$

From the definition (2-10) and the definition of the generalized stress, it is apparent that $T_{ij}=T_{ji}$ and, as a result, only nine components are independent. In addition, the components $T_{iJ}(\boldsymbol{x}_c)$ represent the non-singular part of the generalized stress field at the point $\boldsymbol{x}_c$ and not all these components are unknown a priori. From the continuity of the finite part of the generalized stress at the point $\boldsymbol{x}_c$, it can be readily

verified that the four components T_{12}, T_{22}, T_{23} and T_{24} can be obtained in terms of the generalized crack-face traction at a limiting point $\boldsymbol{x}_c$ on the surface of the crack. As a result, $\{T_{12},T_{22},T_{23},T_{24}\}$, $\{T_{12},T_{22},T_{23}\}$, $\{T_{12},T_{22},T_{23}\}$, and $\{T_{12},T_{23}\}$ are known a priori for electrically impermeable, electrically permeable, electrically semi-permeable, and energetically consistent cracks, respectively. The components T_{22} and T_{24} can be readily obtained once the unknown crack-face generalized tractions are solved. The five independent components $\{T_{11},T_{13},T_{33},T_{14},T_{34}\}$ are always unknown and they are commonly termed the generalized T-stress components. The first three components $\{T_{11},T_{13},T_{33}\}$ are the mechanical T-stress components associated with the stress field similar to the elastic case (see also the work of Rungamornrat and Pinitpanich (2016)) whereas the last two components $\{T_{14},T_{34}\}$ are the electrical T-stress components associated with the electric induction field. The generalized T-stress can be obtained if the generalized stress field at least in the region embedding the crack front is known.

From the near-front asymptotic expansion of the generalized stress field (2-9) and the definition (2-10), components of the generalized T-stress are given explicitly in terms of the generalized stress field by

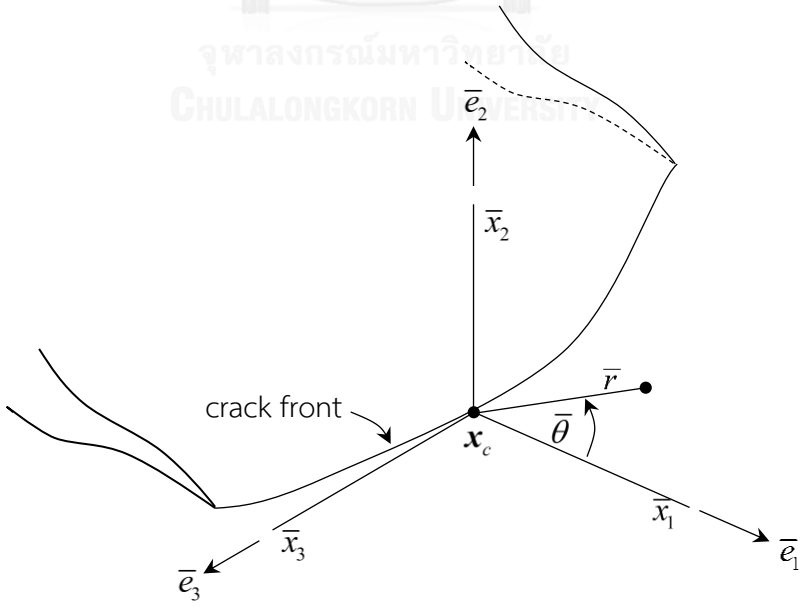

Figure 2-7: Schematic of crack front and local reference coordinate system for defining generalized T-stress components

$$T_Q(\boldsymbol{x}_c) = 2\lim_{\bar{r}\to 0}\sqrt{\bar{r}}\,\frac{\partial}{\partial \bar{r}}\sqrt{\bar{r}}\,\bar{\sigma}_Q(\boldsymbol{x}_c;\bar{r},\bar{\theta}=0) \tag{2-11}$$

where $Q \in \{11,13,33,14,34\}$. According to the formula (2-11), it becomes evident that the generalized T-stress components can be calculated from existing generalized stress fields of a cracked body via standard differentiations and limiting processes without directly carrying the series expansion.

2.5 Existing Generalized Stress Fields

It is apparent from the earlier section that the generalized stress field is the key ingredient for extracting the generalized T-stress. To construct the complete analytical solution for the generalized stress field, various analytical techniques based on the integral transforms, the representation theories, and potential-function-based theories have been applied successfully for cracked bodies with simple crack and domain geometries and loading conditions as recognized in the literature. In the present investigation, existing complete solutions of the generalized stress field for a circular crack embedded in a three-dimensional, transversely isotropic, linear piezoelectric, whole space subjected to four different crack-face conditions are utilized as the basis for the derivation of the generalized T-stress components for various scenarios:

- An impermeable crack: Chen and Shioya (1999) applied the potential-function-based theory to derive the closed-form solution of the generalized stress field of a penny-shaped crack in a three-dimensional piezoelectric whole space under a pair of self-equilibrated, normal concentrated forces and a pair of self-equilibrated concentrated electric charges acting on both crack surfaces. For the special case of uniform remote mechanical and electrical loading, Chen et al. (2000) utilized the potential-function-based theory together with superposition method to derive the closed-form solution of the generalized stress field.
- A permeable crack: Chen and Lim (2005) applied the potential-function-based theory to obtain the analytical solution of the generalized stress field of a circular crack in a three-dimensional, piezoelectric whole space under a pair

of opposite, unit normal, concentrated forces and uniform remote mechanical and electrical loading conditions.

- A semi-permeable crack: Li and Lee (2004b) employed the Hankel integral transform technique to obtain the exact solution of the generalized stress field of a circular crack in a three-dimensional piezoelectric whole space under uniform remote mechanical and electrical loading conditions.
- An energetically consistent crack: Li et al. (2011) applied the classical complex potential theory to derive the generalized stress field of a circular crack contained in a three-dimensional, piezoelectric whole space under uniform remote electrical and mechanical loading conditions.

2.6 Generalized T-stress for General Generalized Traction

The generalized T-stress Green's functions obtained from equation (2-11) for the electrically impermeable and permeable circular cracks are utilized along with the superposition method to construct an integral formula for computing the generalized T-stress components of circular cracks under general, crack-face, normal traction and general, crack-face, surface electrical charge for the impermeable case and under arbitrarily distributed, surface electric charge for the permeable case.

For the impermeable case, let us consider a circular crack under general, self-equilibrated, crack-face, normal traction $t_3^+ = -t_3^-$ and surface electrical charge $t_4^+ = -t_4^-$. The generalized T-stress components for this case, denoted by T_Q for $Q \in \{11,13,33,14,34\}$, can be obtained in an integral form as

$$T_Q(\theta) = \int_{-\pi}^{\pi}\int_{0}^{a} T_Q^{GP}(\theta; r_1, \theta_1)\, t_3^+(t_1, \theta_1) r_1 dr_1 d\theta_1 + \int_{-\pi}^{\pi}\int_{0}^{a} T_Q^{GE}(\theta; r_2, \theta_2)\, t_4^+(r_2, \theta_2) r_2 dr_2 d\theta_2 \qquad (2\text{-}12)$$

where T_Q^{GP} is the generalized T-stress Green's function due to a pair of opposite, unit normal concentrated forces under the impermeable crack-face boundary condition and T_Q^{GE} is the generalized T-stress Green's function due a pair of opposite, unit concentrated electrical charges under the impermeable crack-face boundary condition.

For the permeable case, consider a circular crack under a general, self-equilibrated, crack-face, normal traction $t_3^+ = -t_3^-$. By following the same methodology as that for the impermeable case, the integral formula of the generalized T-stress components is then obtained as

$$T_Q(\theta) = \int_{-\pi}^{\pi}\int_{0}^{a} \bar{T}_Q^{GP}(\theta; r_1, \theta_1)\, t_3^+(t_1, \theta_1) r_1 dr_1 d\theta \tag{2-13}$$

where $\bar{T}_Q^{GP}$ is the generalized T-stress Green's function due to a pair of opposite, unit normal concentrated forces under the electrically permeable crack-face boundary condition.

Chapter 3

DETERMINATION OF GENERALIZED T-STRESS COMPONENTS

By applying the formula (2-11) along with existing solutions of the generalized stress field indicated in Chapter 2, the direct differentiations, and proper limiting procedure, the generalized T-stress components can be derived in an exact form involving only elementary functions. It is noted that the generalized stress field of cracked media under the remote loading can be readily related to that of the cracked medium under an equivalent crack-face generalized traction via the method of superposition. This chapter mainly presents the exact solutions of the generalized T-stress components under four different crack-face conditions and the Green's functions for the generalized T-stress components for both impermeable and permeable crack-face conditions. Finally, the integral formula of the generalized T-stress components for both electrically impermeable and permeable cracks under general loading conditions is presented.

3.1 Generalized T-stress of Impermeable Crack under Uniform Load

The generalized stress fields proposed by Chen and Shioya (1999) are applied together with the methodology described in the previous chapter to provide the generalized T-stress components for an impermeable circular crack under the uniform remote electrical inductions $\{d_1^\infty, d_2^\infty, d_3^\infty\}$, the uniform remote triaxial stresses $\{\sigma_{11}^\infty, \sigma_{22}^\infty, \sigma_{33}^\infty\}$, and the self-equilibrated, uniform normal traction t_3^0 and self-equilibrated uniform electrical charge d_3^0 on the crack surface. The final set of results is given explicitly as

$$T_{11} = -4\pi^2 A\left\{\sum_{i=1}^{3}\left[\left(c_{66}-c_{11}\right)+c_{13}s_i\alpha_{i1}+e_{31}s_i\alpha_{i2}\right]p_i\right\}+\bar{\sigma}_{11}^\infty \tag{3-1}$$

$$T_{33} = -4\pi^2 A\left\{\sum_{i=1}^{3}\left[\left(c_{66}-c_{11}\right)+c_{13}s_i\alpha_{i1}+e_{31}s_i\alpha_{i2}\right]p_i\right\}+\bar{\sigma}_{33}^\infty \tag{3-2}$$

$$T_{13} = \bar{\sigma}_{13}^\infty,\ T_{14} = \bar{d}_1^\infty,\ T_{34} = \bar{d}_3^\infty \tag{3-3}$$

where $\{\bar{\sigma}_{11}^\infty, \bar{\sigma}_{13}^\infty, \bar{\sigma}_{33}^\infty\}$ and $\{\bar{d}_1^\infty, \bar{d}_3^\infty\}$ are components of the remote triaxial stresses and remote electrical inductions referring to the local coordinate system defined in

Section 2.4 and all involved quantities are given by

$$A = 1/4\pi^2 (g_1 g_4 - g_2 g_3) \tag{3-4}$$

$$p_i = (d_i g_3 - c_i g_4)(\sigma_{33}^{\infty} + t_3^0) + (c_i g_2 - d_i g_1)(d_3^{\infty} + d_3^0) \tag{3-5}$$

$$g_1 = -\sum_{i=1}^{3} c_i \gamma_{i1} \tag{3-6}$$

$$g_2 = -\sum_{i=1}^{3} d_i \gamma_{i1} \tag{3-7}$$

$$g_3 = -\sum_{i=1}^{3} c_i \gamma_{i2} \tag{3-8}$$

$$g_4 = -\sum_{i=1}^{3} d_i \gamma_{i2} \tag{3-9}$$

$$\begin{Bmatrix} c_1 \\ c_2 \\ c_3 \end{Bmatrix} = \frac{1}{2\pi} \begin{bmatrix} s_1 & s_2 & s_3 \\ \alpha_{11} & \alpha_{21} & \alpha_{31} \\ \alpha_{12} & \alpha_{22} & \alpha_{32} \end{bmatrix}^{-1} \begin{Bmatrix} 1 \\ -1 \\ 0 \end{Bmatrix} \tag{3-10}$$

$$\begin{Bmatrix} d_1 \\ d_2 \\ d_3 \end{Bmatrix} = \frac{1}{2\pi} \begin{bmatrix} s_1 & s_2 & s_3 \\ \alpha_{11} & \alpha_{21} & \alpha_{31} \\ \alpha_{12} & \alpha_{22} & \alpha_{32} \end{bmatrix}^{-1} \begin{Bmatrix} e_{15}/c_{44} \\ 0 \\ -1 \end{Bmatrix} \tag{3-11}$$

$$\gamma_{i1} = -c_{13} + c_{33} s_i \alpha_{i1} + e_{33} s_i \alpha_{i2} \tag{3-12}$$

$$\gamma_{i2} = -e_{31} + e_{33} s_i \alpha_{i1} - \varepsilon_{33} s_i \alpha_{i2} \tag{3-13}$$

$$\alpha_{i1} = \frac{c_{11}\varepsilon_{11} - m_3 s_i^2 + c_{44}\varepsilon_{33} s_i^4}{\left(m_1 - m_2 s_i^2\right) s_i} \tag{3-14}$$

$$\alpha_{i2} = \frac{c_{11} e_{15} - m_4 s_i^2 + c_{44} e_{33} s_i^4}{\left(m_1 - m_2 s_i^2\right) s_i} \tag{3-15}$$

$$m_1 = \varepsilon_{11}\left(c_{13} + c_{44}\right) + e_{15}\left(e_{15} + e_{31}\right) \tag{3-16}$$

$$m_2 = \varepsilon_{33}\left(c_{13} + c_{44}\right) + e_{33}\left(e_{15} + e_{31}\right) \tag{3-17}$$

$$m_3 = c_{11}\varepsilon_{33} + c_{44}\varepsilon_{11} + \left(e_{15} + e_{31}\right)^2 \tag{3-18}$$

$$m_4 = c_{11} e_{33} + c_{44} e_{15} - \left(c_{13} + c_{44}\right)\left(e_{15} + e_{31}\right) \tag{3-19}$$

$$s_4^2 = c_{66}/c_{44} \tag{3-20}$$

All involved material constants are defined by $c_{11} = E_{1111}$, $c_{13} = E_{1133}$, $c_{33} = E_{3333}$, $c_{44} = E_{1313}$, $c_{66} = E_{1212}$, $e_{15} = E_{1341}$, $e_{31} = E_{1143}$, $e_{33} = E_{3343}$, $\varepsilon_{11} = -E_{1441}$, $\varepsilon_{33} = -E_{3443}$ and the three parameters $\{s_1^2, s_2^2, s_3^2\}$ are solutions of the nonlinear equation

$$as^6 - bs^4 + cs^2 - d = 0 \tag{3-21}$$

where constants a, b, c, d are defined by

$$a = c_{44}\left(e_{33}^2 + c_{33}\varepsilon_{33}\right) \tag{3-22}$$

$$b = c_{33}m_3 + \varepsilon_{33}\left[c_{44}^2 - \left(c_{13} + c_{44}\right)^2\right] + e_{33}\left(2m_4 - c_{11}e_{33}\right) \tag{3-23}$$

$$c = c_{44}m_3 + \varepsilon_{11}\left[c_{11}c_{33} - \left(c_{13} + c_{44}\right)^2\right] + e_{15}\left(2m_4 - c_{44}e_{15}\right) \tag{3-24}$$

$$d = c_{11}\left(e_{15}^2 + c_{44}\varepsilon_{11}\right) \tag{3-25}$$

All involved parameters given above can be also found in the work of Chen and Shioya (1999).

3.2 Generalized T-stress of Permeable Crack under Uniform Load

By using the generalized stress field proposed by Chen and Lim (2005) along with the same procedure utilized in Section 3.1, the closed-form solution of the generalized T-stress components for an electrically permeable circular crack under the uniform remote triaxial stresses $\{\sigma_{11}^{\infty}, \sigma_{22}^{\infty}, \sigma_{33}^{\infty}\}$, the uniform remote electrical inductions $\{d_1^{\infty}, d_2^{\infty}, d_3^{\infty}\}$, and the self-equilibrated, crack-face, uniform normal traction t_3^0 can be obtained as

$$T_{11} = \frac{\sigma_{33}^{\infty} + t_3^0}{g_1}\sum_{i=1}^{3}\left[\left(c_{66} - c_{11}\right) + c_{13}s_i\alpha_{i1} + e_{31}s_i\alpha_{i2}\right]c_i + \bar{\sigma}_{11}^{\infty} \tag{3-26}$$

$$T_{33} = \frac{\sigma_{33}^{\infty} + t_3^0}{g_1}\sum_{i=1}^{3}\left[\left(c_{66} - c_{11}\right) + c_{13}s_i\alpha_{i1} + e_{31}s_i\alpha_{i2}\right]c_i + \bar{\sigma}_{33}^{\infty} \tag{3-27}$$

$$T_{13} = \bar{\sigma}_{13}^{\infty},\ T_{14} = \bar{d}_1^{\infty},\ T_{34} = \bar{d}_3^{\infty} \tag{3-28}$$

where parameter c_i are given by

$$\begin{Bmatrix} c_1 \\ c_2 \\ c_3 \end{Bmatrix} = -\frac{1}{2\pi}\begin{bmatrix} \gamma_{11}s_1 & \gamma_{21}s_2 & \gamma_{31}s_3 \\ \alpha_{11} & \alpha_{21} & \alpha_{31} \\ \alpha_{12} & \alpha_{22} & \alpha_{32} \end{bmatrix}^{-1}\begin{Bmatrix} 0 \\ 1 \\ 0 \end{Bmatrix} \tag{3-29}$$

and all remaining parameters are defined in the same fashion as those provided in Section 3.1 (the definition of all parameters can be also found in the work of Chen and Lim (2005)).

3.3 Generalized T-stress of Semi-permeable Crack under Uniform Load

By starting with results reported in Li and Lee (2004b), the generalized T-stress components for an electrically semi-permeable circular crack under the uniform remote tri-axial stresses $\{\sigma_{11}^{\infty},\sigma_{22}^{\infty},\sigma_{33}^{\infty}\}$, the uniform remote electrical inductions $\{d_1^{\infty},d_2^{\infty},d_3^{\infty}\}$, and the self-equilibrated, crack-face, uniform normal traction t_3^0 can be obtained explicitly as

$$T_{11}=\frac{-P}{2\kappa}\sum_{i=1}^{3}\left[2\beta_{0i}a_i+\left(c_{11}-c_{12}\right)a_i\right]+\bar{\sigma}_{11}^{\infty} \tag{3-30}$$

$$T_{33}=\frac{-P}{2\kappa}\sum_{i=1}^{3}\left[2\beta_{5i}a_i-\left(c_{11}-c_{12}\right)a_i\right]+\bar{\sigma}_{33}^{\infty} \tag{3-31}$$

$$T_{13}=\bar{\sigma}_{13}^{\infty},\ T_{14}=\bar{d}_1^{\infty},\ T_{34}=\bar{d}_3^{\infty} \tag{3-32}$$

where all involved parameters are defined by

$$P=\begin{cases}d_3^{\infty}-d_3^{c}, & \sigma_{33}^{\infty}=t_3^0=0\\ \sigma_{33}^{\infty}+t_3^0, & \sigma_{33}^{\infty}\neq 0 \text{ or } t_3^0\neq 0\end{cases} \tag{3-33}$$

$$\kappa=\begin{cases}\displaystyle\sum_{j=1}^{3}\beta_{4j}a_j, & \sigma_{33}^{\infty}=t_3^0=0\\ \displaystyle\sum_{j=1}^{3}\beta_{1j}a_j, & \sigma_{33}^{\infty}\neq 0 \text{ or } t_3^0\neq 0\end{cases} \tag{3-34}$$

$$\begin{Bmatrix}a_2/a_1\\ a_3/a_1\end{Bmatrix}=-\left(\mathbf{A}^T\right)^{-1}\mathbf{B} \tag{3-35}$$

$$\mathbf{A}=\begin{bmatrix}\beta_{22} & (\sigma_{33}^{\infty}+t_3^0)\beta_{42}+(d_3^{c}-d_3^{\infty})\beta_{12}\\ \beta_{23} & (\sigma_{33}^{\infty}+t_3^0)\beta_{43}+(d_3^{c}-d_3^{\infty})\beta_{13}\end{bmatrix} \tag{3-36}$$

$$\mathbf{B}=\begin{Bmatrix}\beta_{21}\\ (\sigma_{33}^{\infty}+t_3^0)\beta_{41}+(d_3^{c}-d_3^{\infty})\beta_{11}\end{Bmatrix} \tag{3-37}$$

$$d_3^{c}=\frac{-m_1\pm\sqrt{m_1^2-4m_0m_2}}{2m_2} \tag{3-38}$$

$$m_0=\varepsilon_c(\sigma_{33}^{\infty}+t_3^0)\det\left[\boldsymbol{\beta}_4\quad\boldsymbol{\beta}_2\quad\boldsymbol{\eta}_2\right]-\varepsilon_c d_3^{\infty}\det\left[\boldsymbol{\beta}_1\quad\boldsymbol{\beta}_2\quad\boldsymbol{\eta}_2\right] \tag{3-39}$$

$$m_1=\varepsilon_c\det\left[\boldsymbol{\beta}_1\quad\boldsymbol{\beta}_2\quad\boldsymbol{\eta}_2\right]+(\sigma_{33}^{\infty}+t_3^0)\det\left[\boldsymbol{\beta}_4\quad\boldsymbol{\beta}_2\quad\boldsymbol{\eta}_1\right]-d_3^{\infty}\det\left[\boldsymbol{\beta}_1\quad\boldsymbol{\beta}_2\quad\boldsymbol{\eta}_1\right] \tag{3-40}$$

$$m_2=\det\left[\boldsymbol{\beta}_1\quad\boldsymbol{\beta}_2\quad\boldsymbol{\eta}_1\right] \tag{3-41}$$

$$\boldsymbol{\beta}_k = \begin{Bmatrix} \beta_{k1} \\ \beta_{k2} \\ \beta_{k3} \end{Bmatrix}, k = 1, 2, 4 \tag{3-42}$$

$$\boldsymbol{\eta}_{k-2} = \begin{Bmatrix} \eta_{k1}\gamma_1 \\ \eta_{k2}\gamma_2 \\ \eta_{k3}\gamma_3 \end{Bmatrix}, k = 3, 4 \tag{3-43}$$

$$\beta_{0j} = \left(c_{13}\eta_{3j} + e_{31}\eta_{4j}\right)\gamma_j^2 - c_{11} \tag{3-44}$$

$$\beta_{1j} = \left(c_{33}\eta_{3j} + e_{33}\eta_{4j}\right)\gamma_j^2 - c_{13} \tag{3-45}$$

$$\beta_{2j} = \left[c_{44}\left(1+\eta_{3j}\right) + e_{15}\eta_{4j}\right]\gamma_j \tag{3-46}$$

$$\beta_{3j} = \left[e_{15}\left(1+\eta_{3j}\right) - \varepsilon_{11}\eta_{4j}\right]\gamma_j \tag{3-47}$$

$$\beta_{4j} = \left(e_{33}\eta_{3j} - \varepsilon_{33}\eta_{4j}\right)\gamma_j^2 - e_{31} \tag{3-48}$$

$$\beta_{5j} = \left(c_{13}\eta_{3j} + e_{31}\eta_{4j}\right)\gamma_j^2 - c_{12} \tag{3-49}$$

with ε_c denoting the dielectric permittivity of a medium filled within the crack cavity and γ_j^2, η_{3j} and η_{4j} for j = 1, 2, 3 being solved from the two nonlinear algebraic equations

$$\gamma_j^2 = \frac{c_{11}}{c_{44} + \left(c_{13} + c_{44}\right)\eta_{3j} + \left(e_{31} + e_{15}\right)\eta_{4j}} = \frac{c_{13} + c_{44} + c_{44}\eta_{3j} + e_{15}\eta_{4j}}{c_{33}\eta_{3j} + e_{33}\eta_{4j}} \tag{3-50}$$

$$\gamma_j^2 = \frac{c_{11}}{c_{44} + \left(c_{13} + c_{44}\right)\eta_{3j} + \left(e_{31} + e_{15}\right)\eta_{4j}} = \frac{e_{31} + e_{15} + e_{15}\eta_{3j} - \varepsilon_{11}\eta_{4j}}{e_{33}\eta_{3j} - \varepsilon_{33}\eta_{4j}} \tag{3-51}$$

The equation (3-50) & (3-51) can be further reduced to a cubic equation in terms of γ_j^2:

$$a_0(\gamma_j^2)^3 + b_0(\gamma_j^2)^2 + c_0(\gamma_j^2) + d_0 = 0 \tag{3-52}$$

where a_0, b_0, c_0, d_0 are constants given by

$$a_0 = c_{44}(c_{33}\varepsilon_{33} + e_{33}^2) \tag{3-53}$$

$$\begin{aligned} b_0 = {} & -c_{33}c_{44}\varepsilon_{11} + c_{13}^2\varepsilon_{33} - c_{11}c_{33}\varepsilon_{33} + 2c_{13}c_{44}\varepsilon_{33} - c_{33}e_{15}^2 \\ & -c_{11}e_{33}^2 - 2c_{33}e_{31}e_{15} - c_{33}e_{31}^2 + 2c_{13}e_{33}e_{15} + 2c_{13}e_{33}e_{31} \\ & +2c_{44}e_{33}e_{31} \end{aligned} \tag{3-54}$$

$$\begin{aligned} c_0 = {} & -c_{13}^2\varepsilon_{11} + c_{11}c_{33}\varepsilon_{11} - 2c_{13}c_{44}\varepsilon_{11} + c_{11}c_{44}\varepsilon_{33} - 2c_{13}e_{15}^2 \\ & -2c_{13}e_{15}e_{31} + c_{44}e_{31}^2 + 2c_{11}e_{15}e_{33} \end{aligned} \tag{3-55}$$

$$d_0 = -c_{11}(c_{44}\varepsilon_{11} + e_{15}^2) \tag{3-56}$$

It should be remarked that only the value of d_3^c computed from (3-38) that falls between those of the two limiting cases (i.e., electrically permeable and electrically impermeable cases) is acceptable. Remark that the closed-form solution of the semi-permeable model can be further reduced to the special cases of impermeable and permeable models by taking the dielectric permittivity of the crack medium within the crack cavity ε_c to zero and infinity, respectively.

3.4 Generalized T-stress of Energetically Consistent Crack under Uniform Load

The generalized T-stress components for an energetically consistent circular crack under the uniform remote triaxial stresses $\{\sigma_{11}^{\infty}, \sigma_{22}^{\infty}, \sigma_{33}^{\infty}\}$ and the uniform remote electrical inductions $\{d_1^{\infty}, d_2^{\infty}, d_3^{\infty}\}$ can be derived using the same procedure and the analytical solution presented by Li et al. (2011). Final results are given explicitly by

$$T_{11} = \frac{\pi i}{4}\sum_{j=1}^{3} A_j \left[\left(c_{11} + c_{12}\right) - \frac{2\left(c_{13}k_{2j} - e_{31}k_{1j}\right)}{v_j^2} \right] + \bar{\sigma}_{11}^{\infty} \tag{3-57}$$

$$T_{33} = \frac{\pi i}{4}\sum_{j=1}^{3} A_j \left[\left(c_{11} + c_{12}\right) - \frac{2\left(c_{13}k_{2j} - e_{31}k_{1j}\right)}{v_j^2} \right] + \bar{\sigma}_{33}^{\infty} \tag{3-58}$$

$$T_{13} = \bar{\sigma}_{13}^{\infty},\ T_{14} = \bar{d}_1^{\infty},\ T_{34} = \bar{d}_3^{\infty} \tag{3-59}$$

where all involved parameters are defined by (also see the work of Li et al. (2011))

$$A_j = \Lambda_{j2}\left[\sigma_{33}^{\infty} - \frac{(d_3^c)^2}{2\varepsilon_c} \right] + \Lambda_{j3}(d_3^{\infty} - d_3^c) \tag{3-60}$$

$$H_1 = \pi\sum_{j=1}^{3} \frac{k_{2j}}{v_j}\Lambda_{j2} \tag{3-61}$$

$$H_2 = \pi\sum_{j=1}^{3} \frac{k_{2j}}{v_j}\Lambda_{j3} \tag{3-62}$$

$$H_3 = -\pi\sum_{j=1}^{3} \frac{k_{1j}}{v_j}\Lambda_{j2} \tag{3-63}$$

$$H_4 = -\pi\sum_{j=1}^{3} \frac{k_{1j}}{v_j}\Lambda_{j3} \tag{3-64}$$

$$d_3^c = -\varepsilon_c \frac{H_3\left[\sigma_{33}^{\infty} - \dfrac{(d_3^c)^2}{2\varepsilon_c}\right] + H_4(d_3^{\infty} - d_3^c)}{H_1\left[\sigma_{33}^{\infty} - \dfrac{(d_3^c)^2}{2\varepsilon_c}\right] + H_2(d_3^{\infty} - d_3^c)} \tag{3-65}$$

$$\mathbf{\Lambda} = \mathbf{B}^{-1} \tag{3-66}$$

$$B_{1j} = \frac{1}{v_j}\left[c_{44}(1+k_{2j}) - e_{15}k_{1j}\right] \tag{3-67}$$

$$B_{2j} = \frac{\pi i}{2}\left[c_{44}(1+k_{2j}) - e_{15}k_{1j}\right] \tag{3-68}$$

$$B_{3j} = \frac{\pi i}{2}\left[e_{44}(1+k_{2j}) + \varepsilon_{11}k_{1j}\right] \tag{3-69}$$

with v_j, k_{1j} and k_{2j} obtained from

$$v_j^2 = \frac{c_{44} + (c_{13}+c_{44})k_{2j} - (e_{31}+e_{15})k_{1j}}{c_{11}} = \frac{c_{33}k_{2j} - e_{33}k_{1j}}{(c_{13}+c_{44}) + c_{44}k_{2j} - e_{15}k_{1j}} \tag{3-70}$$

$$v_j^2 = \frac{c_{44} + (c_{13}+c_{44})k_{2j} - (e_{31}+e_{15})k_{1j}}{c_{11}} = \frac{e_{33}k_{2j} + \varepsilon_{33}k_{1j}}{(e_{15}+e_{31}) + \varepsilon_{11}k_{1j} + e_{15}k_{2j}} \tag{3-71}$$

It is also important to remark that d_3^c computed from (3-65) is acceptable if it induces a positive value of the crack-opening displacement. Remark that the analytical solution associated with the energetically consistent model can be further specialized to the solutions of impermeable and permeable crack-face conditions by taking the dielectric permittivity of a medium within the crack cavity ε_c to zero and infinity, respectively.

3.5 Generalized T-stress Green's Function for Impermeable Crack

Consider a problem concerning a circular crack under a pair of opposite, unit normal point forces and electric point charges as reported by Chen and Shioya (1999). The closed-form solution of the generalized-stress Green's function is given by

$$\sigma_1^G = 8A\sum_{j=1}^{3}\left[(c_{66}-c_{11}) + c_{13}s_j\alpha_{j1} + e_{31}s_j\alpha_{j2}\right]\left[\beta_{j1}f_{31}(z_j) + \beta_{j2}f_{32}(z_j)\right] \tag{3-72}$$

$$\sigma_2^G = 8Ac_{66}\sum_{j=1}^{3}\left[\beta_{j1}f_{41}(z_j) + \beta_{j2}f_{42}(z_j)\right] \tag{3-73}$$

$$\tau_z^G = 4A\sum_{j=1}^{3}\left[c_{44}(s_j+\alpha_{j1}) + e_{15}\alpha_{j2}\right]\left[\beta_{j1}f_{51}(z_j) + \beta_{j2}f_{52}(z_j)\right] \tag{3-74}$$

$$D^G = 4A\sum_{j=1}^{3}\left[e_{15}\left(s_j+\alpha_{j1}\right)-\varepsilon_{11}\alpha_{j2}\right]\left[\beta_{j1}f_{51}\left(z_j\right)+\beta_{j2}f_{52}\left(z_j\right)\right] \tag{3-75}$$

in which a superscript "G" is used to designate Green's function, $i=\sqrt{-1}$, $z_j = s_j z$,

$$\sigma_1^G = \sigma_{rr}^G + \sigma_{\theta\theta}^G \tag{3-76}$$

$$\sigma_2^G = \left(\sigma_{rr}^G - \sigma_{\theta\theta}^G + 2i\sigma_{r\theta}^G\right)e^{2i\theta} \tag{3-77}$$

$$\tau_z^G = \left(\sigma_{rz}^G + \sigma_{\theta z}^G\right)e^{i\theta} \tag{3-78}$$

$$D^G = \left(D_r^G + D_\theta^G\right)e^{i\theta} \tag{3-79}$$

$$\beta_{j1} = c_j g_4 - d_j g_3 \tag{3-80}$$

$$\beta_{j2} = d_j g_1 - c_j g_2 \tag{3-81}$$

All other involved parameters defined in Section 3.1 apply here and the complex functions $f_{3j}\left(z_j\right), f_{4j}\left(z_j\right), f_{5j}\left(z_j\right)$ are defined by

$$f_{3j}\left(z\right) = \frac{z}{R_j^3}\tan^{-1}\left(\frac{h_j}{R_j}\right) - \frac{h_j}{z\left(R_j^2+h_j^2\right)}\left[\frac{r^2-l_1^2}{l_2^2-l_1^2} - \frac{z^2}{R_j^2}\right] \tag{3-82}$$

$$\begin{aligned} f_{4j}\left(z\right) = {} & \frac{\sqrt{a^2-r_j^2}}{\overline{t}_j\overline{s}_j}\left(\frac{2}{\overline{t}_j} - \frac{r_j e^{i\theta_j}}{\overline{s}_j^2}\right)\tan^{-1}\left[\frac{\overline{s}_j}{\sqrt{l_2^2-a^2}}\right] - \frac{z\left(3R_j^2-z^2\right)}{\overline{t}_j^{\,2}R_j^3}\tan^{-1}\left(\frac{h_j}{R_j}\right) \\ & + \frac{\sqrt{a^2-r_j^2}\sqrt{l_2^2-a^2}\,r_j e^{i\theta_j}}{\overline{t}_j\overline{s}_j^2\left[l_2^2 - rr_j e^{-i\left(\theta-\theta_j\right)}\right]} - \frac{zh_j}{R_j^2+h_j^2}\left[\frac{t_j}{\overline{t}_j R_j^2} - \frac{r^2e^{2i\theta}}{\left(l_2^2-l_1^2\right)\left(l_2^2-r^2\right)}\right] \end{aligned} \tag{3-83}$$

$$f_{5j}\left(z\right) = \frac{t_j}{R_j^3}\tan^{-1}\left(\frac{h_j}{R_j}\right) + \frac{h_j}{R_j^2+h_j^2}\left[\frac{re^{i\theta}}{l_2^2-l_1^2} + \frac{t_j}{R_j^2}\right] \tag{3-84}$$

with all involved parameters defined explicitly by

$$l_1 = \frac{1}{2}\left[\sqrt{\left(r+a\right)^2+z^2} - \sqrt{\left(r-a\right)^2+z^2}\right] \tag{3-85}$$

$$l_2 = \frac{1}{2}\left[\sqrt{\left(r+a\right)^2+z^2} + \sqrt{\left(r-a\right)^2+z^2}\right] \tag{3-86}$$

$$h_j = \frac{\sqrt{a^2-l_1^2}\sqrt{a^2-r_j^2}}{a} \tag{3-87}$$

$$t_j = re^{i\theta} - r_j e^{i\theta_j} \tag{3-88}$$

$$\overline{t}_j = re^{-i\theta} - r_j e^{-i\theta_j} \tag{3-89}$$

$$\overline{s}_j = \sqrt{a^2 - rr_j e^{-i\left(\theta-\theta_j\right)}} \tag{3-90}$$

$$R_j = \sqrt{r^2 + r_j^2 - 2rr_j\cos\left(\theta - \theta_j\right) + z^2} \tag{3-91}$$

By first noting following properties (see also the work of Rungamornrat and Pinitpanich (2016)

$$\lim_{z\to 0}\frac{\sqrt{a-l_1}}{z} = \frac{\sqrt{a}}{\sqrt{2\left(r^2-a^2\right)}} \tag{3-92}$$

$$\lim_{z\to 0}\frac{zh_j}{l_2 - r} = \frac{2\sqrt{r^2-a^2}\sqrt{a^2-r_j^2}}{r} \tag{3-93}$$

and then substituting these results into (3-82)-(3-84) and (3-72)-(3-75), the Green's function for the generalized stress at any point on the plane $z=0$ is given explicitly by

$$\sigma_1^G\left(r,\theta,0;r_\alpha,\theta_\alpha\right) = 8A\sum_{j=1}^{3}\left[\left(c_{66}-c_{11}\right)+c_{13}s_j\alpha_{j1}+e_{31}s_j\alpha_{j2}\right]\left[\beta_{j1}f_{31}(0) + \beta_{j2}f_{32}(0)\right] \tag{3-94}$$

$$\sigma_2^G\left(r,\theta,0;r_\alpha,\theta_\alpha\right) = 8Ac_{66}\sum_{j=1}^{3}\left[\beta_{j1}f_{41}(0)+\beta_{j2}f_{42}(0)\right] \tag{3-95}$$

$$\tau_z^G\left(r,\theta,0;r_\alpha,\theta_\alpha\right) = 0 \tag{3-96}$$

$$D^G\left(r,\theta,0;r_\alpha,\theta_\alpha\right) = 0 \tag{3-97}$$

where $f_{3\alpha}(0),\ f_{4\alpha}(0),\ f_{5\alpha}(0)$ for $\alpha = 1,2$ are given by

$$f_{3\alpha}(0) = -\frac{\sqrt{a^2-r_\alpha^2}}{\sqrt{r^2-a^2}R_{0\alpha}^2} \tag{3-98}$$

$$f_{4\alpha}(0) = \frac{\sqrt{a^2-r_\alpha^2}}{\bar{t}_\alpha\bar{s}_\alpha}\left(\frac{2}{\bar{t}_\alpha}-\frac{r_\alpha e^{i\theta_\alpha}}{\bar{s}_\alpha^2}\right)\tan^{-1}\left(\frac{\bar{s}_\alpha}{\sqrt{r^2-a^2}}\right) + \frac{\sqrt{r^2-a^2}\sqrt{a^2-r_\alpha^2}r_\alpha e^{i\theta_\alpha}}{\bar{t}_\alpha\bar{s}_\alpha^2\left(r^2-rr_\alpha e^{-i(\theta-\theta_\alpha)}\right)} + \frac{e^{2i\theta}\sqrt{a^2-r_\alpha^2}}{R_{0\alpha}^2\sqrt{r^2-a^2}} \tag{3-99}$$

$$f_{5\alpha}(0) = 0 \tag{3-100}$$

with the parameter $R_{0\alpha}$ given by

$$R_{0\alpha} = R_\alpha\left(z=0\right) = \sqrt{r^2+r_\alpha^2-2rr_\alpha\cos\left(\theta-\theta_\alpha\right)} \tag{3-101}$$

By introducing the variable transformation $\bar{r} = r - a$ together with the proper limiting process, for $(r_\alpha, \theta_\alpha) \neq (a, \theta)$, it is readily to show that

$$\lim_{\bar{r}\to 0}\left\{\sqrt{\bar{r}}\,\frac{\partial}{\partial \hat{r}}\left[\sqrt{\bar{r}}\left(\frac{\sqrt{a^2-r_\alpha^2}}{\sqrt{r^2-a^2}}\right)\right]\right\} = 0 \tag{3-102}$$

$$\lim_{\bar{r}\to 0}\left\{\sqrt{\bar{r}}\,\frac{\partial}{\partial \hat{r}}\left[\sqrt{\bar{r}}\left(\frac{\sqrt{r^2-a^2}\sqrt{a^2-r_\alpha^2}}{\bar{t}_\alpha \bar{s}_\alpha^2\left(r^2 - r r_\alpha e^{-i(\theta-\theta_\alpha)}\right)}\right)\right]\right\} = 0 \tag{3-103}$$

$$\begin{aligned}\lim_{\bar{r}\to 0}\left\{\sqrt{\bar{r}}\,\frac{\partial}{\partial \hat{r}}\left[\sqrt{\bar{r}}\left(\frac{\sqrt{a^2-r_\alpha^2}}{\bar{t}_\alpha \bar{s}_\alpha}\left(\frac{2}{\bar{t}_\alpha} - \frac{r_\alpha e^{i\theta_\alpha}}{\bar{s}_\alpha^2}\right)\tan^{-1}\left(\frac{\bar{s}_\alpha}{\sqrt{r^2-a^2}}\right)\right)\right]\right\} \\ = \pi\sqrt{a^2-r_\alpha^2}\left(\frac{1}{2\bar{t}_{0\alpha}^2\bar{s}_{0\alpha}} - \frac{r_\alpha e^{i\theta_\alpha}}{4\bar{t}_{0\alpha}\bar{s}_{0\alpha}^3}\right)\end{aligned} \tag{3-104}$$

where $\bar{t}_{0\alpha} = ae^{-i\theta} - r_\alpha e^{-i\theta_\alpha}$ and $\bar{s}_{0\alpha} = \sqrt{a^2 - a r_\alpha e^{-i(\theta-\theta_\alpha)}}$. By substituting (3-102)-(3-104) into (3-98)-(3-100) and (2-11) along with the relations (3-76)-(3-79), the generalized T-stress components are obtained as

$$\begin{aligned}T_{11}^G(\theta; r_\alpha, \theta_\alpha) = 4\pi A c_{66}\sum_{j=1}^{3}\sum_{\alpha=1}^{2}\Re\left[\beta_{j\alpha}\left(\frac{\sqrt{a^2-r_\alpha^2}}{\sqrt{a}\left(ae^{-i\theta} - r_\alpha e^{-i\theta_\alpha}\right)\sqrt{a - r_\alpha e^{-i(\theta-\theta_\alpha)}}}\right)\right. \\ \left.\times\left(\frac{1}{a - r_\alpha e^{-i(\theta_\alpha-\theta)}} - \frac{r_\alpha e^{i(\theta_\alpha-\theta)}}{2a\left(a - r_\alpha e^{-i(\theta-\theta_\alpha)}\right)}\right)\right]\end{aligned} \tag{3-105}$$

$$\begin{aligned}T_{33}^G(\theta; r_\alpha, \theta_\alpha) = 4\pi A c_{66}\sum_{j=1}^{3}\sum_{\alpha=1}^{2}\Re\left[\beta_{j\alpha}\left(\frac{\sqrt{a^2-r_\alpha^2}}{\sqrt{a}\left(ae^{-i\theta} - r_\alpha e^{-i\theta_\alpha}\right)\sqrt{a - r_\alpha e^{-i(\theta-\theta_\alpha)}}}\right)\right. \\ \left.\times\left(\frac{r_\alpha e^{i(\theta_\alpha-\theta)}}{2a\left(a - r_\alpha e^{-i(\theta-\theta_\alpha)}\right)} - \frac{1}{a - r_\alpha e^{-i(\theta_\alpha-\theta)}}\right)\right]\end{aligned} \tag{3-106}$$

$$\begin{aligned}T_{13}^G(\theta; r_\alpha, \theta_\alpha) = 4\pi A c_{66}\sum_{j=1}^{3}\sum_{\alpha=1}^{2}\Im\left[\beta_{j\alpha}\left(\frac{\sqrt{a^2-r_\alpha^2}}{\sqrt{a}\left(ae^{-i\theta} - r_\alpha e^{-i\theta_\alpha}\right)\sqrt{a - r_\alpha e^{-i(\theta-\theta_\alpha)}}}\right)\right. \\ \left.\times\left(\frac{1}{a - r_\alpha e^{-i(\theta_\alpha-\theta)}} - \frac{r_\alpha e^{i(\theta_\alpha-\theta)}}{2a\left(a - r_\alpha e^{-i(\theta-\theta_\alpha)}\right)}\right)\right]\end{aligned} \tag{3-107}$$

$$T_{14}^{G} = 0 \tag{3-108}$$

$$T_{34}^{G} = 0 \tag{3-109}$$

where $\Re(f)$ and $\Im(f)$ represent real and imaginary parts of a complex function f, respectively. The expressions (3-105)-(3-107) can be reduced further by introducing new variables l_1, l_2, ϕ_1, ϕ_2 satisfying

$$\begin{aligned} r_1 \sin(\theta_1 - \theta) &= l_1 \sin\phi \\ r_1 \cos(\theta_1 - \theta) + l_1 \cos\phi &= a \end{aligned} \tag{3-110}$$

$$\begin{aligned} r_2 \sin(\theta_2 - \theta) &= l_2 \sin\phi \\ r_2 \cos(\theta_2 - \theta) + l_2 \cos\phi &= a \end{aligned} \tag{3-111}$$

and $\beta_{j\alpha} = A_{j\alpha} + iB_{j\alpha}$ where $A_{j\alpha}$ and $B_{j\alpha}$ are real and imaginary parts of $\beta_{j\alpha}$. The graphical interpretation of the new variables l_1, l_2, ϕ_1, ϕ_2 is indicated in Figure 3-1.

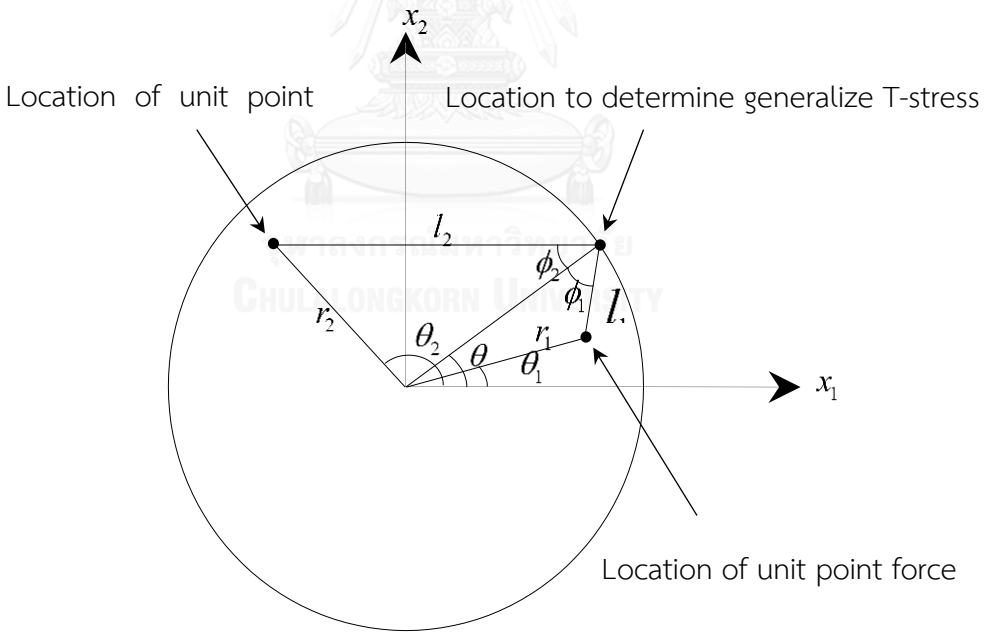

Figure 3-1: Graphical interpretation of variables $r_1, r_2, l_1, l_2, \theta_1, \theta_2, \theta$, ϕ_1, and ϕ_2

The final form of the generalized T-stress Green's function is now given by

$$T_Q^G = T_Q^{GP} + T_Q^{GE} \tag{3-112}$$

where T_Q^{GP} and T_Q^{GE} are components of the generalized T-stress Green's function due to a pair of opposite, unit normal concentrated forces and a pair of opposite, unit concentrated, electrical charges, respectively. The explicit expressions of both T_Q^{GP} and T_Q^{GE} are given by

$$T_{11}^{GP}(\theta,l_1,\phi_1)=-4\pi Ac_{66}\frac{1}{l_1^2}\sqrt{2\cos\phi_1-\frac{l_1}{a}}\left\{\left[\frac{1}{2}\left(1-\frac{l_1}{a}\right)\cos\frac{\phi_1}{2}-\cos\frac{3\phi_1}{2}\right]\sum_{j=1}^{3}A_{j1}-\left[\frac{1}{2}\left(1+\frac{l_1}{a}\right)\sin\frac{\phi_1}{2}+\sin\frac{3\phi_1}{2}\right]\sum_{j=1}^{3}B_{j1}\right\} \tag{3-113}$$

$$T_{33}^{GP}(\theta,l_1,\phi_1)=4\pi Ac_{66}\frac{1}{l_1^2}\sqrt{2\cos\phi_1-\frac{l_1}{a}}\left\{\left[\frac{1}{2}\left(1-\frac{l_1}{a}\right)\cos\frac{\phi_1}{2}-\cos\frac{3\phi_1}{2}\right]\sum_{j=1}^{3}A_{j1}-\left[\frac{1}{2}\left(1+\frac{l_1}{a}\right)\sin\frac{\phi_1}{2}+\sin\frac{3\phi_1}{2}\right]\sum_{j=1}^{3}B_{j1}\right\} \tag{3-114}$$

$$T_{13}^{GP}(\theta,l_1,\phi_1)==-4\pi Ac_{66}\frac{1}{l_1^2}\sqrt{2\cos\phi_1-\frac{l_1}{a}}\left\{\left[\frac{1}{2}\left(1-\frac{l_1}{a}\right)\cos\frac{\phi_1}{2}-\cos\frac{3\phi_1}{2}\right]\sum_{j=1}^{3}B_{j1}+\left[\frac{1}{2}\left(1+\frac{l_1}{a}\right)\sin\frac{\phi_1}{2}+\sin\frac{3\phi_1}{2}\right]\sum_{j=1}^{3}A_{j1}\right\} \tag{3-115}$$

$$T_{11}^{GE}(\theta,l_2,\phi_2)=-4\pi Ac_{66}\frac{1}{l_2^2}\sqrt{2\cos\phi_2-\frac{l_2}{a}}\left\{\left[\frac{1}{2}\left(1-\frac{l_2}{a}\right)\cos\frac{\phi_2}{2}-\cos\frac{3\phi_2}{2}\right]\sum_{j=1}^{3}A_{j2}-\left[\frac{1}{2}\left(1+\frac{l_2}{a}\right)\sin\frac{\phi_2}{2}+\sin\frac{3\phi_2}{2}\right]\sum_{j=1}^{3}B_{j2}\right\} \tag{3-116}$$

$$T_{33}^{GE}(\theta,l_2,\phi_2)=4\pi Ac_{66}\frac{1}{l_2^2}\sqrt{2\cos\phi_2-\frac{l_2}{a}}\left\{\left[\frac{1}{2}\left(1-\frac{l_2}{a}\right)\cos\frac{\phi_2}{2}-\cos\frac{3\phi_2}{2}\right]\sum_{j=1}^{3}A_{j2}-\left[\frac{1}{2}\left(1+\frac{l_2}{a}\right)\sin\frac{\phi_2}{2}+\sin\frac{3\phi_2}{2}\right]\sum_{j=1}^{3}B_{j2}\right\} \tag{3-117}$$

$$T_{13}^{GE}(\theta,l_2,\phi_2)=-4\pi Ac_{66}\frac{1}{l_2^2}\sqrt{2\cos\phi_2-\frac{l_2}{a}}\left\{\left[\frac{1}{2}\left(1-\frac{l_2}{a}\right)\cos\frac{\phi_2}{2}-\cos\frac{3\phi_2}{2}\right]\sum_{j=1}^{3}B_{j2}+\left[\frac{1}{2}\left(1+\frac{l_2}{a}\right)\sin\frac{\phi_2}{2}+\sin\frac{3\phi_2}{2}\right]\sum_{j=1}^{3}A_{j2}\right\} \tag{3-118}$$

From the formula (3-113)-(3-118), it is apparent that the generalized T-stress Green's functions of an impermeable crack depend on material properties and are singular only at $l=0$ of $\mathcal{O}\left(1/l^2\right)$.

3.6 Generalized T-stress Green's Function for Permeable Crack

Consider, next, a circular crack under a pair of opposite, unit normal point forces presented by Chen and Lim (2005), the exact solution of the generalized stress Green's function is given by

$$\sigma_{z3}^{G} = \frac{1}{g_1\pi^2}\sum_{j=1}^{3}\gamma_{j3}c_j f_3\left(z_j\right) \tag{3-119}$$

$$\sigma_{2}^{G} = \frac{2c_{66}}{g_1\pi^2}\sum_{j=1}^{3}c_j f_4\left(z_j\right) \tag{3-120}$$

$$\tau_{z1}^{G} = \frac{1}{g_1\pi^2}\sum_{j=1}^{3}\gamma_{j1}s_j c_j f_5\left(z_j\right) \tag{3-121}$$

$$\tau_{z2}^{G} = \frac{1}{g_1\pi^2}\sum_{j=1}^{3}\gamma_{j2}s_j c_j f_5\left(z_j\right) \tag{3-122}$$

where $\sigma_1^G, \sigma_2^G, \tau_{z1}^G, \tau_{z2}^G$ and γ_{j1}, γ_{j2}, γ_{j3} are defined by

$$\sigma_1^G = \sigma_{rr}^G + \sigma_{\theta\theta}^G \tag{3-123}$$

$$\sigma_2^G = \left(\sigma_{rr}^G - \sigma_{\theta\theta}^G + 2i\sigma_{r\theta}^G\right)e^{2i\theta} \tag{3-124}$$

$$\tau_{z1}^G = \left(\sigma_{rz}^G + \sigma_{\theta z}^G\right)e^{i\theta} \tag{3-125}$$

$$\tau_{z2}^G = \left(D_r^G + D_\theta^G\right)e^{i\theta} \tag{3-126}$$

$$\gamma_{j1} = -c_{13} + c_{33}s_j\alpha_{j1} + e_{33}s_j\alpha_{j2} \tag{3-127}$$

$$\gamma_{j2} = -e_{31} + e_{33}s_j\alpha_{j1} - \varepsilon_{33}s_j\alpha_{j2} \tag{3-128}$$

$$\gamma_{j3} = 2\left[\left(c_{66} - c_{11}\right) + c_{13}s_j\alpha_{j1} + e_{31}s_j\alpha_{j2}\right] \tag{3-129}$$

All other involved parameters defined in Section 3.1 apply here except c_j are defined in Section 3.2 and the complex functions $f_3\left(z_j\right), f_4\left(z_j\right), f_5\left(z_j\right)$ are given explicitly by

$$f_3\left(z\right) = \frac{z}{R_0^3}\tan^{-1}\left(\frac{h}{R_0}\right) - \frac{h}{z\left(R_0^2+h^2\right)}\left[\frac{r^2-l_1^2}{l_2^2-l_1^2} - \frac{z^2}{R_0^2}\right] \tag{3-130}$$

$$\begin{aligned} f_4\left(z\right) = {} & \frac{\sqrt{a^2-r_0^2}}{\bar{t}\,\bar{s}}\left(\frac{2}{\bar{t}} - \frac{r_0e^{i\theta_0}}{\bar{s}^2}\right)\tan^{-1}\left[\frac{\bar{s}}{\sqrt{l_2^2-a^2}}\right] - \frac{z\left(3R_0^2-z^2\right)}{\bar{t}^{\,2}R_0^3}\tan^{-1}\left(\frac{h}{R_0}\right) \\ & + \frac{\sqrt{a^2-r_0^2}\sqrt{l_2^2-a^2}\,r_0e^{i\theta_0}}{\bar{t}\,\bar{s}^2\left[l_2^2 - rr_0e^{-i(\theta-\theta_0)}\right]} - \frac{zh}{R_0^2+h^2}\left[\frac{t}{\bar{t}R_0^2} - \frac{r^2e^{2i\theta}}{\left(l_2^2-l_1^2\right)\left(l_2^2-r^2\right)}\right] \end{aligned} \tag{3-131}$$

$$f_4(z)=\frac{t}{R_0^3}\tan^{-1}\left(\frac{h}{R_0}\right)+\frac{h}{R_0^2+h^2}\left[\frac{re^{i\theta}}{l_2^2-l_1^2}+\frac{t}{R_0^2}\right] \tag{3-132}$$

where

$$h=\frac{\sqrt{a^2-l_1^2}\sqrt{a^2-r_0^2}}{a} \tag{3-133}$$

$$t=re^{i\theta}-r_0e^{i\theta_0} \tag{3-134}$$

$$\overline{s}=\sqrt{a^2-rr_0e^{-i(\theta-\theta_0)}} \tag{3-135}$$

$$R_0=\sqrt{r^2+r_0^2-2rr_0\cos(\theta-\theta_0)+z^2} \tag{3-136}$$

By applying the properties (3-92)-(3-93) to the relations (3-130)-(3-132) and (3-119)-(3-122) , the Green's function of the generalized stress at any point on the plane $z=0$ is given by

$$\sigma_{z3}^G(r,\theta,0;r_0,\theta_0)=\frac{1}{g_1\pi^2}\sum_{j=1}^{3}\gamma_{j3}c_j f_3(0) \tag{3-137}$$

$$\sigma_2^G(r,\theta,0;r_0,\theta_0)=\frac{2c_{66}}{g_1\pi^2}\sum_{j=1}^{3}c_j f_4(0) \tag{3-138}$$

$$\tau_{z1}^G(r,\theta,0;r_0,\theta_0)=0 \tag{3-139}$$

$$\tau_{z2}^G(r,\theta,0;r_0,\theta_0)=0 \tag{3-140}$$

where g_1 is defined in Section 3.1, and $f_3(0),\ f_4(0),\ f_5(0)$ are obtained as

$$f_3(0)=-\frac{\sqrt{a^2-r_0^2}}{\sqrt{r^2-a^2}R_{00}^2} \tag{3-141}$$

$$f_4(0)=\frac{\sqrt{a^2-r_0^2}}{\overline{t}_0\overline{s}_0}\left(\frac{2}{\overline{t}_0}-\frac{r_0e^{i\theta_0}}{\overline{s}_0^2}\right)\tan^{-1}\left(\frac{\overline{s}_0}{\sqrt{r^2-a^2}}\right)+\frac{\sqrt{r^2-a^2}\sqrt{a^2-r_0^2}r_0e^{i\theta_0}}{\overline{t}_0\overline{s}_0^2\left(r^2-rr_0e^{-i(\theta-\theta_0)}\right)} \tag{3-142}$$

$$+\frac{e^{2i\theta}\sqrt{a^2-r_0^2}}{R_{00}^2\sqrt{r^2-a^2}}$$

$$f_5(0)=0 \tag{3-143}$$

with R_{00} defined by

$$R_{00}=R_0(z=0)=\sqrt{r^2+r_0^2-2rr_0\cos(\theta-\theta_0)} \tag{3-144}$$

By introducing, again, the variable transformation $\bar{r} = r - a$ along with the proper limiting process, it can be proved, for $(r_0, \theta_0) \neq (a, \theta)$, that

$$\lim_{\bar{r}\to 0}\left\{\sqrt{\bar{r}}\,\frac{\partial}{\partial \hat{r}}\left[\sqrt{\bar{r}}\left(\frac{\sqrt{a^2-r_0^2}}{\sqrt{r^2-a^2}}\right)\right]\right\} = 0 \tag{3-145}$$

$$\lim_{\bar{r}\to 0}\left\{\sqrt{\bar{r}}\,\frac{\partial}{\partial \hat{r}}\left[\sqrt{\bar{r}}\left(\frac{\sqrt{r^2-a^2}\sqrt{a^2-r_0^2}}{\bar{t}\,\bar{s}^2\left(r^2 - rr_0e^{-i(\theta-\theta_0)}\right)}\right)\right]\right\} = 0 \tag{3-146}$$

$$\lim_{\bar{r}\to 0}\left\{\sqrt{\bar{r}}\,\frac{\partial}{\partial \bar{r}}\left[\sqrt{\bar{r}}\left(\frac{\sqrt{a^2-r_\alpha^2}}{\bar{t}\,\bar{s}}\left(\frac{2}{\bar{t}} - \frac{r_0e^{i\theta_0}}{\bar{s}^2}\right)\tan^{-1}\left(\frac{\bar{s}}{\sqrt{r^2-a^2}}\right)\right)\right]\right\} = \pi\sqrt{a^2-r_\alpha^2}\left(\frac{1}{2\bar{t}_0^{\,2}\bar{s}_0} - \frac{r_0e^{i\theta_0}}{4\bar{t}_0\bar{s}_0^3}\right) \tag{3-147}$$

where $\bar{t}_0 = ae^{-i\theta} - r_0e^{-i\theta_0}$ and $\bar{s}_0 = \sqrt{a^2 - ar_0e^{-i(\theta-\theta_0)}}$. By substituting the results (3-145)-(3-147) into (3-137)-(3-140), (2-11), and (3-123)-(3-126), the generalized T-stress Green's functions are obtained as

$$T_{11}^G(\theta, r_0, \theta_0) = \frac{c_{66}}{g_1\pi}\sum_{j=1}^{3}\Re\left[c_j\left(\frac{\sqrt{a^2-r_0^2}}{\sqrt{a}\left(ae^{-i\theta} - r_0e^{-i\theta_0}\right)\sqrt{a - r_0e^{-i(\theta-\theta_0)}}}\right)\times\left(\frac{1}{a - r_0e^{-i(\theta_0-\theta)}} - \frac{r_0e^{i(\theta_0-\theta)}}{2a\left(a - r_0e^{-i(\theta-\theta_0)}\right)}\right)\right] \tag{3-148}$$

$$T_{33}^G(\theta, r_0, \theta_0) = \frac{c_{66}}{g_1\pi}\sum_{j=1}^{3}\Re\left[c_j\left(\frac{\sqrt{a^2-r_0^2}}{\sqrt{a}\left(ae^{-i\theta} - r_0e^{-i\theta_0}\right)\sqrt{a - r_0e^{-i(\theta-\theta_0)}}}\right)\times\left(\frac{r_0e^{i(\theta_0-\theta)}}{2a\left(a - r_0e^{-i(\theta-\theta_0)}\right)} - \frac{1}{a - r_0e^{-i(\theta_0-\theta)}}\right)\right] \tag{3-149}$$

$$T_{13}^G(\theta, r_0, \theta_0) = \frac{c_{66}}{g_1\pi}\sum_{j=1}^{3}\Im\left[c_j\left(\frac{\sqrt{a^2-r_0^2}}{\sqrt{a}\left(ae^{-i\theta} - r_0e^{-i\theta_0}\right)\sqrt{a - r_0e^{-i(\theta-\theta_0)}}}\right)\times\left(\frac{1}{a - r_0e^{-i(\theta_0-\theta)}} - \frac{r_1e^{i(\theta_0-\theta)}}{2a\left(a - r_0e^{-i(\theta-\theta_0)}\right)}\right)\right] \tag{3-150}$$

$$T_{14}^{G}=0 \tag{3-151}$$

$$T_{34}^{G}=0 \tag{3-152}$$

The expressions (3-148)-(3-150) can be further reduced by introducing the following variable transformations

$$\begin{aligned} r_0\sin\left(\theta_0-\theta\right)&=l\sin\phi\\ r_0\cos\left(\theta_0-\theta\right)+l\cos\phi&=a \end{aligned} \tag{3-153}$$

and the representation $c_j=A_j+iB_j$ where A_j and B_j are real and imaginary parts of c_j. The graphical interpretation of the variables l,ϕ is indicated in Figure 3-2. The generalized T-stress Green's function can be given explicitly by

$$\begin{aligned} T_{11}^{G}\left(\theta,l,\phi\right)=-\frac{c_{66}}{g_1\pi l^2}\sqrt{2\cos\phi-\frac{l}{a}}\Bigg\{&\left[\frac{1}{2}\left(1-\frac{l}{a}\right)\cos\frac{\phi}{2}-\cos\frac{3\phi}{2}\right]\sum_{j=1}^{3}A_j\\ &-\left[\frac{1}{2}\left(1+\frac{l}{a}\right)\sin\frac{\phi}{2}+\sin\frac{3\phi}{2}\right]\sum_{j=1}^{3}B_j\Bigg\} \end{aligned} \tag{3-154}$$

$$\begin{aligned} T_{33}^{G}\left(\theta,l,\phi\right)=\frac{c_{66}}{g_1\pi l^2}\sqrt{2\cos\phi-\frac{l}{a}}\Bigg\{&\left[\frac{1}{2}\left(1-\frac{l}{a}\right)\cos\frac{\phi}{2}-\cos\frac{3\phi}{2}\right]\sum_{j=1}^{3}A_j\\ &-\left[\frac{1}{2}\left(1+\frac{l}{a}\right)\sin\frac{\phi}{2}+\sin\frac{3\phi}{2}\right]\sum_{j=1}^{3}B_j\Bigg\} \end{aligned} \tag{3-155}$$

$$\begin{aligned} T_{13}^{G}\left(\theta,l,\phi\right)=-\frac{c_{66}}{g_1\pi l^2}\sqrt{2\cos\phi-\frac{l}{a}}\Bigg\{&\left[\frac{1}{2}\left(1-\frac{l}{a}\right)\cos\frac{\phi}{2}-\cos\frac{3\phi}{2}\right]\sum_{j=1}^{3}B_j\\ &+\left[\frac{1}{2}\left(1+\frac{l}{a}\right)\sin\frac{\phi}{2}+\sin\frac{3\phi}{2}\right]\sum_{j=1}^{3}A_j\Bigg\} \end{aligned} \tag{3-156}$$

It is clear that the generalized T-stress Green's functions of an electrically permeable crack also depend on material properties and are singular at $l=0$ of $\mathcal{O}\left(1/l^2\right)$.

3.7 Generalized T-stress Components for General Crack-face Loading

Results of the generalized T-stress Green's function established in Section 3.5 and Section 3.6 are employed as a basis to formulate the general integral formula for computing the generalized T-stress components for a circular crack subjected to general crack-face loads.

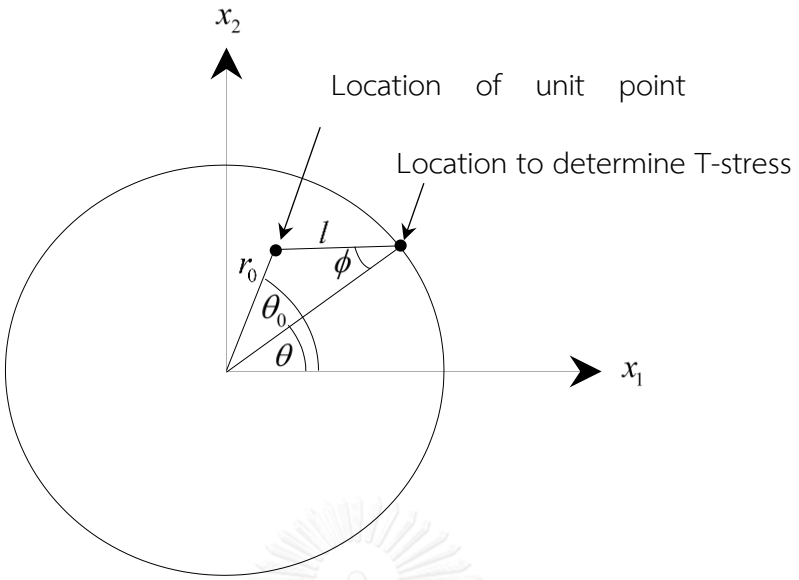

Figure 3-2: Graphical interpretation of variables r_0, l, θ_0, θ and ϕ

3.7.1 Generalized T-stress Components for Impermeable Crack

For an impermeable circular crack under the uniform remote triaxial stresses $\{\sigma_{11}^{\infty}, \sigma_{22}^{\infty}, \sigma_{33}^{\infty}\}$, the uniform remote electrical inductions $\{d_1^{\infty}, d_2^{\infty}, d_3^{\infty}\}$, and the self-equilibrated, crack-face, general normal traction t_3 and the self-equilibrated, crack-face, general electrical charge d_3, the integral formula for the generalized T-stress components is given implicitly by

$$\begin{aligned}\bar{\sigma}_{iJ}\left(\theta,\bar{r},\bar{\theta}\right) = \bar{\sigma}_{iJ}^{\infty} &+ \int_{-\pi}^{\pi}\int_{0}^{a} \bar{\sigma}_{iJ}^{GP}\left(\theta,\bar{r},\bar{\theta};r_1,\theta_1\right)\left\{t_3\left(r_1,\theta_1\right)+\sigma_{33}^{\infty}\right\} r_1 dr_1 d\theta_1 \\ &+ \int_{-\pi}^{\pi}\int_{0}^{a} \bar{\sigma}_{iJ}^{GE}\left(\theta,\bar{r},\bar{\theta};r_2,\theta_2\right)\left\{d_3\left(r_2,\theta_2\right)+d_3^{\infty}\right\} r_2 dr_2 d\theta_2\end{aligned} \tag{3-157}$$

where $\bar{\sigma}_{iJ}$, $\bar{\sigma}_{iJ}^{\infty}$, $\bar{\sigma}_{iJ}^{GP}$, and $\bar{\sigma}_{iJ}^{GE}$ are local components of the generalized stress field, local components of the uniform remote triaxial generalized stresses σ_{iJ}^{∞} (including the remote triaxial stress $\{\sigma_{11}^{\infty}, \sigma_{22}^{\infty}, \sigma_{33}^{\infty}\}$ and remote electrical inductions $\{d_1^{\infty}, d_2^{\infty}, d_3^{\infty}\}$), components of the generalized stress Green's function $\boldsymbol{\sigma}^{GP}$ and $\boldsymbol{\sigma}^{GE}$ under a pair of opposite, unit normal point forces and opposite, unit point charges, respectively. By following the work of Rungamornrat and Pinitpanich (2016), i.e.,

employing equation (2-11) together with the expression (3-157), the generalized T-stress components at any point $(a,\theta,0)$ along the crack front is given by

$$T_Q(\theta)=T_Q^{\infty}+T_Q^{0}(\theta)+T_Q^{1}(\theta) \tag{3-158}$$

with T_Q^{∞}, $T_Q^{0}(\theta)$, and $T_Q^{1}(\theta)$ defined by

$$\begin{aligned}T_Q^{\infty}=\bar{\sigma}_Q^{\infty}&+2\lim_{\bar{r}\to 0}\left\{\sqrt{\bar{r}}\,\frac{\partial}{\partial\bar{r}}\left[\sqrt{\bar{r}}\int_{-\pi}^{\pi}\int_{0}^{a}\bar{\sigma}_Q^{GP}\left(\theta,\bar{r},\bar{\theta};r_1,\theta_1\right)\sigma_{33}^{\infty}r_1dr_1d\theta_1\right]\right\}\\&+2\lim_{\bar{r}\to 0}\left\{\sqrt{\bar{r}}\,\frac{\partial}{\partial\bar{r}}\left[\sqrt{\bar{r}}\int_{-\pi}^{\pi}\int_{0}^{a}\bar{\sigma}_Q^{GE}\left(\theta,\bar{r},\bar{\theta};r_2,\theta_2\right)d_3^{\infty}r_2dr_2d\theta_2\right]\right\}\end{aligned} \tag{3-159}$$

$$\begin{aligned}T_Q^{0}(\theta)=2\lim_{\bar{r}\to 0}&\left\{\sqrt{\bar{r}}\,\frac{\partial}{\partial\bar{r}}\left[\sqrt{\bar{r}}\int_{-\pi}^{\pi}\int_{0}^{a}\bar{\sigma}_Q^{GP}\left(\theta,\bar{r},\bar{\theta};r_1,\theta_1\right)t_3\left(r_1,\theta_1\right)r_1dr_1d\theta_1\right]\right\}\\&+2\lim_{\bar{r}\to 0}\left\{\sqrt{\bar{r}}\,\frac{\partial}{\partial\bar{r}}\left[\sqrt{\bar{r}}\int_{-\pi}^{\pi}\int_{0}^{a}\bar{\sigma}_Q^{GE}\left(\theta,\bar{r},\bar{\theta};r_2,\theta_2\right)d_3\left(r_2,\theta_2\right)r_2dr_2d\theta_2\right]\right\}\end{aligned} \tag{3-160}$$

$$\begin{aligned}T_Q^{1}(\theta)=2\lim_{\bar{r}\to 0}&\left\{\sqrt{\bar{r}}\,\frac{\partial}{\partial\bar{r}}\left[\sqrt{\bar{r}}\int_{-\pi}^{\pi}\int_{0}^{a}\bar{\sigma}_Q^{GP}\left(\theta,\bar{r},\bar{\theta};r_1,\theta_1\right)\left[t_3\left(r_1,\theta_1\right)-t_3\left(a,\theta\right)\right]r_1dr_1d\theta_1\right]\right\}\\&+2\lim_{\bar{r}\to 0}\left\{\sqrt{\bar{r}}\,\frac{\partial}{\partial\bar{r}}\left[\sqrt{\bar{r}}\int_{-\pi}^{\pi}\int_{0}^{a}\bar{\sigma}_Q^{GE}\left(\theta,\bar{r},\bar{\theta};r_2,\theta_2\right)\left[d_3\left(r_2,\theta_2\right)-d_3\left(a,\theta\right)\right]r_2dr_2d\theta_2\right]\right\}\end{aligned} \tag{3-161}$$

where T_Q^{∞} represents the generalized T-stress components associated with the uniform remote triaxial stress σ_{iJ}^{∞}; $T_Q^{0}(\theta)$ are the generalized T-stress components corresponding to the uniform portion of the general applied traction $t_3\left(r_1,\theta_1\right)$ and general electrical charge $d_3\left(r_2,\theta_2\right)$ with the magnitude equal to $t_3\left(r_1=a,\theta_1=\theta\right)$ and $d_3\left(r_2=a,\theta_2=\theta\right)$, respectively; and $T_Q^{1}(\theta)$ represent the generalized T-stress components associated with the remaining portion of the general applied traction $t_3\left(r_1,\theta_1\right)$ and the general electrical charge $d_3\left(r_2,\theta_2\right)$ with its magnitude equal to zero at the point (a,θ), respectively.

By employing the condition $t_3\left(r_1,\theta_1\right)-t_3\left(a,\theta\right)=0$, $d_3\left(r_2,\theta_2\right)-d_3\left(a,\theta\right)=0$ at the point (a,θ) and the fact that the singularity of $\bar{\sigma}_Q^{G}\left(r,\theta,0;r_\alpha,\theta_\alpha\right)$ is present only at a location where the concentrated load is applied together with interchanging the order of limits, integrations and differentiations, the generalized T-stress $T_Q^{1}(\theta)$ can be obtained as

$$T_Q^1(\theta)=\int_{-\pi}^{\pi}\int_0^a\left\{2\lim_{\bar{r}\to 0}\sqrt{\bar{r}}\,\frac{\partial}{\partial\bar{r}}\left[\sqrt{\bar{r}}\,\bar{\sigma}_Q^{GP}\left(\theta,\bar{r},\bar{\theta};r_1,\theta_1\right)\right]\right\}\left[t_3(r_1,\theta_1)-t_3(a,\theta)\right]r_1dr_1d\theta_1$$
$$+\int_{-\pi}^{\pi}\int_0^a\left\{2\lim_{\bar{r}\to 0}\sqrt{\bar{r}}\,\frac{\partial}{\partial\bar{r}}\left[\sqrt{\bar{r}}\,\bar{\sigma}_Q^{GE}\left(\theta,\bar{r},\bar{\theta};r_2,\theta_2\right)\right]\right\}\left[d_3(r_2,\theta_2)-d_3(a,\theta)\right]r_2dr_2d\theta_2 \quad (3\text{-}162)$$

By applying the definition of the generalized T-stress, the relation (3-162) reduces to

$$T_Q^1(\theta)=\int_{-\pi}^{\pi}\int_0^a T_Q^{GP}(\theta;r_1,\theta_1)p_1(r_1,\theta_1)r_1dr_1d\theta_1$$
$$+\int_{-\pi}^{\pi}\int_0^a T_Q^{GE}(\theta;r_2,\theta_2)p_2(r_2,\theta_2)r_2dr_2d\theta_2 \quad (3\text{-}163)$$

where $p_1(r_1,\theta_1)=t_3(r_1,\theta_1)-t_3(a,\theta)$ and $p_2(r_2,\theta_2)=d_3(r_2,\theta_2)-d_3(a,\theta)$. By applying the variable transformations (3-110)-(3-111), it leads to the alternative form of (3-163)

$$T_Q^1(\theta)=\int_{-\pi/2}^{\pi/2}\int_0^{2a\cos\phi}\left[\left(l\hat{T}_Q^{GP}(\theta;l_1,\phi_1)\right)\hat{p}_1(l_1,\phi_1)dl_1d\phi_1\right]$$
$$+\int_{-\pi/2}^{\pi/2}\int_0^{2a\cos\phi}\left[\left(l\hat{T}_Q^{GE}(\theta;l_2,\phi_2)\right)\hat{p}_2(l_2,\phi_2)dl_2d\phi_2\right] \quad (3\text{-}164)$$

where $\hat{p}_1(l_1,\phi_1)=p_1\left(r_1(l_1,\phi_1),\theta_1(l_1,\phi_1)\right)$ and $\hat{p}_2(l_2,\phi_2)=p_2\left(r_2(l_2,\phi_2),\theta_2(l_2,\phi_2)\right)$.

It should be evident from the formula (3-113)-(3-118) that the function $l\hat{T}_Q^{GP}(\theta;l_1,\phi_1)$ and $l\hat{T}_Q^{GE}(\theta;l_2,\phi_2)$ appearing in (3-164) is singular only at $l=0$ of $\mathcal{O}(1/l)$, $\hat{p}_1(0,\phi_1)=0$ and $\hat{p}_2(0,\phi_2)=0$. Moreover, the normal traction $t_3(r_1,\theta_1)$ and the normal electric induction $d_3(r_2,\theta_2)$ are the most important factors for the existence of the integral (3-164). If the functions $t_3(r_1,\theta_1)$ and $d_3(r_2,\theta_2)$ are sufficiently smooth at a point (a,θ) with $\hat{p}_1(l_1,\phi_1)=O\left(l^{\lambda_1}\right)$, $\hat{p}_2(l_2,\phi_2)=O\left(l^{\lambda_2}\right)$, and $\lambda_1,\lambda_2>0$, the existence of all integrals appearing in (3-164) is confirmed since all involved integrands are of $\mathcal{O}\left(l^{\lambda_1-1}\right)$ and $\mathcal{O}\left(l^{\lambda_2-1}\right)$. For $\lambda_1,\lambda_2\geq 1$, all involved integrands are obviously nonsingular and all integrals can be efficiently evaluated by Gaussian quadrature. For $0<\lambda_1,\lambda_2<1$, the involved integrands are weakly singular and a numerical integration technique indicated below is employed. By introducing

the change of variables $l_1 = l_1\left(\bar{l}_1\right) = \bar{l}^{\,\gamma_1}$ and $l_2 = l_2\left(\bar{l}_2\right) = \bar{l}^{\,\gamma_2}$ where γ_1 and γ_2 are selected constants, the integral (3-164) can be modified as

$$\begin{aligned} T_Q^1(\theta) = \gamma_1 \int_{-\pi/2}^{\pi/2} \int_0^{(2a\cos\phi)^{1/\gamma_1}} \left[l_1\left(\bar{l}_1\right) \hat{T}_Q^{GP}\left(\theta; l_1\left(\bar{l}_1\right), \phi_1\right) \right] \hat{p}\left(l_1\left(\bar{l}_1\right), \phi\right) \left[l_1\left(\bar{l}_1\right) \right]^{(\gamma_1 - 1)/\gamma_1} d\bar{l}_1 d\phi_1 \\ + \gamma_2 \int_{-\pi/2}^{\pi/2} \int_0^{(2a\cos\phi)^{1/\gamma_2}} \left[l_2\left(\bar{l}_2\right) \hat{T}_Q^{GE}\left(\theta; l_2\left(\bar{l}_2\right), \phi_2\right) \right] \hat{p}\left(l_2\left(\bar{l}_2\right), \phi_2\right) \left[l_2\left(\bar{l}_2\right) \right]^{(\gamma_2 - 1)/\gamma_2} d\bar{l}_2 d\phi_2 \end{aligned} \tag{3-165}$$

By setting $\gamma_1 = 1/\lambda_1$ and $\gamma_2 = 1/\lambda_2$, the integral (3-165) now becomes

$$\begin{aligned} T_Q^1(\theta) = \frac{1}{\lambda_1} \int_{-\pi/2}^{\pi/2} \int_0^{(2a\cos\phi)^{\lambda_1}} \left[l_1\left(\bar{l}_1\right) \hat{T}_Q^{GP}\left(\theta; l_1\left(\bar{l}_1\right), \phi_1\right) \right] \hat{p}\left(l_1\left(\bar{l}_1\right), \phi\right) \left[l_1\left(\bar{l}_1\right) \right]^{(1 - \lambda_1)} d\bar{l}_1 d\phi_1 \\ + \frac{1}{\lambda_2} \int_{-\pi/2}^{\pi/2} \int_0^{(2a\cos\phi)^{\lambda_2}} \left[l_2\left(\bar{l}_2\right) \hat{T}_Q^{GE}\left(\theta; l_2\left(\bar{l}_2\right), \phi_2\right) \right] \hat{p}\left(l_2\left(\bar{l}_2\right), \phi_2\right) \left[l_2\left(\bar{l}_2\right) \right]^{(1 - \lambda_2)} d\bar{l}_2 d\phi_2 \end{aligned} \tag{3-166}$$

It is apparent that all integrals appearing in (3-166) can now be efficiently integrated by standard Gaussian Quadrature since the weak singularity at $l = 0$ is completely removed by the specific choice of γ_1, γ_2.

Since the closed-form solution of the generalized T-stress of an impermeable circular crack under the uniform remote and crack-face loadings is already established in Section 3.1, the generalized T-stress components T_Q^∞ and $T_Q^0(\theta)$ are then given by

$$T_{11}^\infty = A\left\{ \sum_{i=1}^{3} \left[\left(c_{66} - c_{11}\right) + c_{13} s_i \alpha_{i1} + e_{31} s_i \alpha_{i2} \right] p_i^\infty \right\} + \bar{\sigma}_{11}^\infty \tag{3-167}$$

$$T_{33}^\infty = A\left\{ \sum_{i=1}^{3} \left[\left(c_{66} - c_{11}\right) + c_{13} s_i \alpha_{i1} + e_{31} s_i \alpha_{i2} \right] p_i^\infty \right\} + \bar{\sigma}_{33}^\infty \tag{3-168}$$

$$T_{13}^\infty = \bar{\sigma}_{13}^\infty,\ T_{14}^\infty = \bar{d}_1^\infty,\ T_{34}^\infty = \bar{d}_3^\infty \tag{3-169}$$

$$T_{11}^0 = T_{33}^0 = A\left\{ \sum_{i=1}^{3} \left[\left(c_{66} - c_{11}\right) + c_{13} s_i \alpha_{i1} + e_{31} s_i \alpha_{i2} \right] p_i^0 \right\} \tag{3-170}$$

$$T_{13}^0 = 0,\ T_{14}^0 = 0,\ T_{34}^0 = 0 \tag{3-171}$$

where the loading parameters p_i^0 and p_i^∞ are defined in a fashion similar to those indicated in the relation (3-5), i.e., $p_i^\infty = (d_i g_3 - c_i g_4)\sigma_{33}^\infty + (c_i g_2 - d_i g_1) d_3^\infty$ and $p_i^0 = (d_i g_3 - c_i g_4)\sigma_{33}^0 + (c_i g_2 - d_i g_1) d_3^0$.

3.7.2 Generalized T-stress Components for Permeable Crack

For a permeable circular crack under the uniform remote triaxial stresses $\{\sigma_{11}^{\infty},\sigma_{22}^{\infty},\sigma_{33}^{\infty}\}$, the uniform remote electrical inductions $\{d_1^{\infty},d_2^{\infty},d_3^{\infty}\}$, and the self-equilibrated, crack-face, general normal traction t_3, the integral formula of the generalized T-stress components are given implicitly by

$$\bar{\sigma}_{iJ}\left(\theta,\bar{r},\bar{\theta}\right)=\bar{\sigma}_{iJ}^{\infty}+\int_{-\pi}^{\pi}\int_{0}^{a}\bar{\sigma}_{iJ}^{GP}\left(\theta,\bar{r},\bar{\theta};r_0,\theta_0\right)\left\{t_3\left(r_0,\theta_0\right)+\sigma_{33}^{\infty}\right\}r_0dr_0d\theta_0 \tag{3-172}$$

By following the procedure similar to that employed by Rungamornrat and Pinitpanich (2016), components of the generalized T-stress at any point $(a,\theta,0)$ on the crack boundary can be also written as

$$T_Q\left(\theta\right)=T_Q^{\infty}+T_Q^0\left(\theta\right)+T_Q^1\left(\theta\right) \tag{3-173}$$

where T_Q^{∞}, $T_Q^0\left(\theta\right)$, $T_Q^1\left(\theta\right)$ are defined by

$$T_Q^{\infty}=\bar{\sigma}_Q^{\infty}+2\lim_{\bar{r}\to 0}\left\{\sqrt{\bar{r}}\,\frac{\partial}{\partial\bar{r}}\left[\sqrt{\bar{r}}\int_{-\pi}^{\pi}\int_{0}^{a}\bar{\sigma}_Q^{GP}\left(\theta,\bar{r},\bar{\theta};r_0,\theta_0\right)\sigma_{33}^{\infty}r_0dr_0d\theta_0\right]\right\} \tag{3-174}$$

$$T_Q^0\left(\theta\right)=2\lim_{\bar{r}\to 0}\left\{\sqrt{\bar{r}}\,\frac{\partial}{\partial\bar{r}}\left[\sqrt{\bar{r}}\int_{-\pi}^{\pi}\int_{0}^{a}\bar{\sigma}_Q^{GP}\left(\theta,\bar{r},\bar{\theta};r_0,\theta_0\right)t_3\left(r_0,\theta_0\right)r_0dr_0d\theta_0\right]\right\} \tag{3-175}$$

$$T_Q^1\left(\theta\right)=2\lim_{\bar{r}\to 0}\left\{\sqrt{\bar{r}}\,\frac{\partial}{\partial\bar{r}}\left[\sqrt{\bar{r}}\int_{-\pi}^{\pi}\int_{0}^{a}\bar{\sigma}_Q^{GP}\left(\theta,\bar{r},\bar{\theta};r_0,\theta_0\right)\left[t_3\left(r_0,\theta_0\right)-t_3\left(a,\theta\right)\right]r_0dr_0d\theta_0\right]\right\} \tag{3-176}$$

Note that the meaning of T_Q^{∞}, $T_Q^0\left(\theta\right)$, and $T_Q^1\left(\theta\right)$ is similar to that described in Section 3.7.1.

Again, by employing the condition $t_3\left(r_1,\theta_1\right)-t_3\left(a,\theta\right)=0$ at the point (a,θ) and the fact that the singularity of $\bar{\sigma}_Q^G\left(r,\theta,0;r_\alpha,\theta_\alpha\right)$ is present only at a location where the concentrated force is applied along with the interchange of the order of limits, differentiations and integrations, the generalized T-stress $T_Q^1\left(\theta\right)$ can be obtained as

$$T_Q^1\left(\theta\right)=\int_{-\pi}^{\pi}\int_{0}^{a}\left\{2\lim_{\bar{r}\to 0}\sqrt{\bar{r}}\,\frac{\partial}{\partial\bar{r}}\left[\sqrt{\bar{r}}\,\bar{\sigma}_Q^{GP}\left(\theta,\bar{r},\bar{\theta};r_0,\theta_0\right)\right]\right\}\left[t_3\left(r_0,\theta_0\right)-t_3\left(a,\theta\right)\right]r_0dr_0d\theta_0 \tag{3-177}$$

By utilizing the definition of the generalized T-stress, the expression (3-177) can be simplified to

$$T_Q^1(\theta)=\int_{-\pi}^{\pi}\int_0^a T_Q^{GP}(\theta;r_0,\theta_0)p(r_0,\theta_0)r_0dr_0d\theta_0 \tag{3-178}$$

where $p(r_0,\theta_0)=t_3(r_0,\theta_0)-t_3(a,\theta)$. By applying the variable transformations (3-110)-(3-111) to the integral relation (3-178), it leads to an alternative integral formula

$$T_Q^1(\theta)=\int_{-\pi/2}^{\pi/2}\int_0^{2a\cos\phi}\left[\left(l\hat{T}_Q^{GP}(\theta;l,\phi)\right)\hat{p}(l,\phi)dld\phi\right] \tag{3-179}$$

where $\hat{p}(l,\phi)=p\left(r_0(l,\phi),\theta_0(l,\phi)\right)$. It should be evident from the formula (3-154)-(3-156) that the function $l\hat{T}_Q^{GP}(\theta;l,\phi)$ appearing in (3-179) is singular only at $l=0$ of $\mathcal{O}(1/l)$ and $\hat{p}(0,\phi)=0$. If the traction data $t_3(r_0,\theta_0)$ is sufficiently smooth at a point (a,θ) such that $\hat{p}(l,\phi)=\mathcal{O}(l^{\lambda})$ with $\lambda>0$, the integrand of (3-179) is obviously of $\mathcal{O}(l^{\lambda_1-1})$ and, as a result, the existence of the integral in (3-179) is confirmed. For $\lambda\geq 1$, the integral appearing in (3-179) is clearly not singular and can be integrated using standard Gaussian quadrature while for $0<\lambda<1$, the integral contains a weakly singular integrand and the same integration scheme described in Section 3.7.1 is applied. Specifically, by utilizing the variable transformation $l=l(\bar{l})=\bar{l}^{\gamma}$ where γ denotes a pre-selected constant, the formula (3-179) can be modified as

$$T_Q^1(\theta)=\gamma\int_{-\pi/2}^{\pi/2}\int_0^{(2a\cos\phi)^{1/\gamma}}\left[l(\bar{l})\hat{T}_Q^{GP}\left(\theta;l(\bar{l}),\phi\right)\right]\hat{p}\left(l(\bar{l}),\phi\right)\left[l(\bar{l})\right]^{(\gamma-1)/\gamma}d\bar{l}_0d\phi_0 \tag{3-180}$$

By setting $\gamma=1/\lambda$, (3-180) now becomes

$$T_Q^1(\theta)=\frac{1}{\lambda}\int_{-\pi/2}^{\pi/2}\int_0^{(2a\cos\phi)^{\lambda}}\left[l(\bar{l})\hat{T}_Q^{GP}\left(\theta;l(\bar{l}),\phi\right)\right]\hat{p}\left(l(\bar{l}),\phi\right)\left[l(\bar{l})\right]^{(1-\lambda)}d\bar{l}d\phi \tag{3-181}$$

It is evident that for the chosen γ, the singularity of the integrand at $l=0$ is fully eliminated. Now, the resulting integral can be integrated accurately and efficiently by

standard Gaussian quadrature.

By using the exact solution of the components of the generalized T-stress for a permeable circular crack under uniform remote and crack-face loading presented in Section 3.2, the generalized T-stress components T_Q^{∞} and $T_Q^0(\theta)$ can be given explicitly by

$$T_{33}^{\infty} = (\sigma_{33}^{\infty} / g_1)\sum_{i=1}^{3}\left[(c_{66} - c_{11}) + c_{13}s_i\alpha_{i1} + e_{31}s_i\alpha_{i2}\right]c_i + \bar{\sigma}_{11}^{\infty} \tag{3-182}$$

$$T_{33}^{\infty} = (\sigma_{33}^{\infty} / g_1)\sum_{i=1}^{3}\left[(c_{66} - c_{11}) + c_{13}s_i\alpha_{i1} + e_{31}s_i\alpha_{i2}\right]c_i + \bar{\sigma}_{33}^{\infty} \tag{3-183}$$

$$T_{13}^{\infty} = \bar{\sigma}_{13}^{\infty},\ T_{14}^{\infty} = \bar{d}_1^{\infty},\ T_{34}^{\infty} = \bar{d}_3^{\infty} \tag{3-184}$$

$$T_{11}^{0} = T_{33}^{0} = (t_3^0 / g_1)\sum_{i=1}^{3}\left[(c_{66} - c_{11}) + c_{13}s_i\alpha_{i1} + e_{31}s_i\alpha_{i2}\right]c_i \tag{3-185}$$

$$T_{13}^{0} = 0,\ T_{14}^{0} = 0,\ T_{34}^{0} = 0 \tag{3-186}$$

Chapter 4

NUMERICAL RESULTS

Verification of the integral formula of the generalized T-stress components derived in the previous chapter for impermeable and permeable circular cracks subjected to general crack-face loading conditions is presented in this chapter. In addition, the influence of the crack-face and applied loads on the generalized T-stress along the crack boundary is reported.

4.1 Verification of Integral Formula for Generalized T-stress

Consider impermeable and permeable circular cracks under only the linearly distributed, self-equilibrated, crack-face normal traction $t_3 = \sigma_0 \left(1 + x_1 / a\right) / 2$ along the global x_1-axis (see Figure 4-1). The body is made from a representative transversely isotropic, piezoelectric material with the properties similar to those of PZT-5H, shown in Table 4-1. To verify the integral formula developed in Section 3.7, two benchmark cases are considered. First, the formula (3-158) for the impermeable crack is specialized to an elastic case by simply eliminating the electric-mechanical coupling effect (i.e., $e_{15} = e_{31} = e_{33} = 0$) and results are then compared with the analytical solution reported by Rungamornrat and Pinitpanich (2016) as shown in Figure 4-2. Next, results obtained from the integral formula (3-158) and (3-173) are benchmarked with solutions obtained from a numerical technique presented by Limwibul et al. (2016) in Figure 4-3 and Figure 4-4 for impermeable and permeable cracks, respectively.

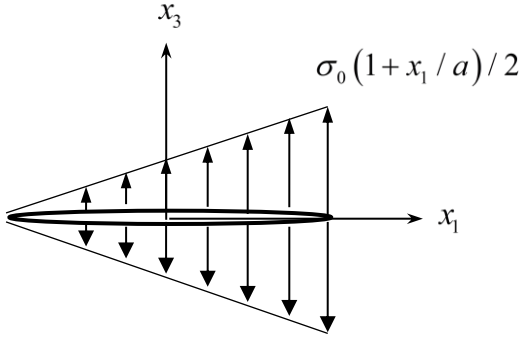

Figure 4-1: Circular crack under linearly distributed, self-equilibrated, crack-face normal traction $\sigma_0 \left(1 + x_1 / a\right) / 2$ along the global x_1-axis

Table 4-1: Elastic moduli, piezoelectric constants and dielectric permittivities of representative, transversely isotropic, piezoelectric solid identical to PZT-5H (eg. Li and Lee (2004b))

Elastic constants (x 10^9 Pa)	c_{11}	126.00
	c_{13}	53.00
	c_{33}	117.00
	c_{44}	35.30
	c_{66}	35.50
Piezoelectric constants (C/m^2)	e_{15}	17.00
	e_{31}	-6.50
	e_{33}	23.30
Dielectric permittivities (x 10^{-9} C/(Vm))	ε_{11}	15.10
	ε_{33}	13.00

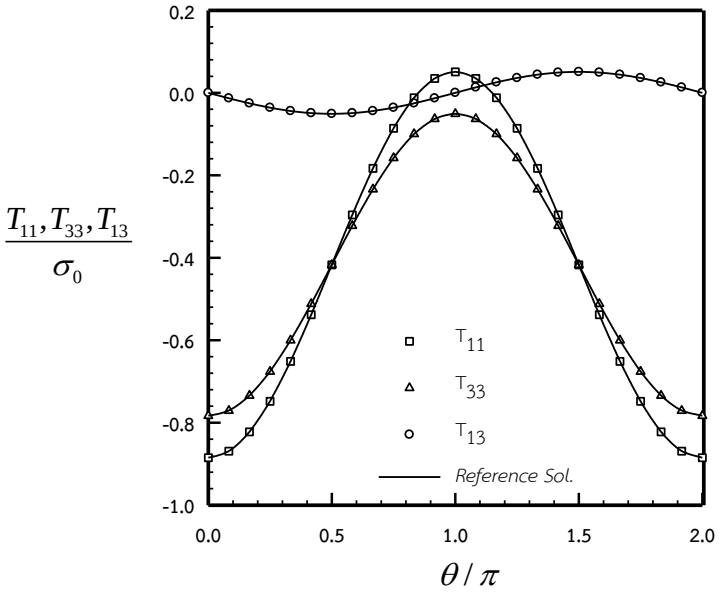

Figure 4-2: Normalized T-stress components of circular crack due to linearly distributed, self-equilibrated, crack-face, normal traction $\sigma_0\left(1+x_1/a\right)/2$ by ignoring the electro-mechanical effect. The reference solution is taken from Rungamornrat and Pinitpanich (2016).

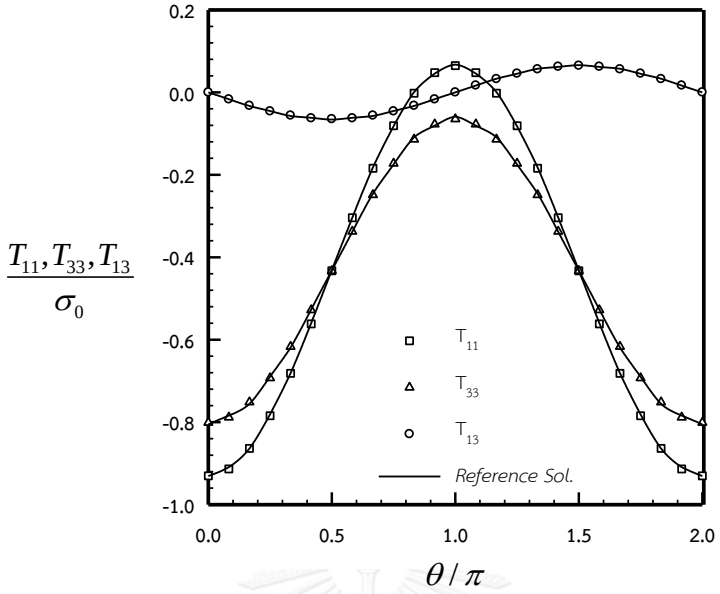

Figure 4-3: Normalized generalized T-stress components of impermeable circular crack subjected to linearly distributed, self-equilibrated, crack-face, normal traction $\sigma_0 \left(1 + x_1 / a\right) / 2$. The reference solution is generated by a technique proposed by Limwibul et al. (2016).

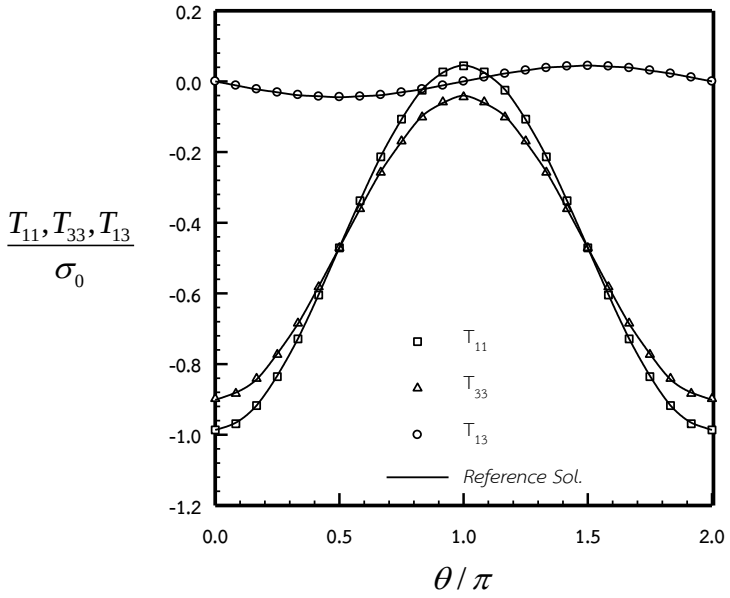

Figure 4-4: Normalized generalized T-stress components of permeable circular crack subjected to linearly distributed, self-equilibrated, crack-face, normal traction $\sigma_0 \left(1 + x_1 / a\right) / 2$. The benchmark solutions are obtained from numerical technique developed by Limwibul et al. (2016).

It is evident from these results that numerical solutions generated by the proposed integral formula exhibit an excellent agreement with the reference solutions for both cases. This good agreement of results should ensure the correctness of both the proposed integral formula and the implemented numerical quadrature.

4.2 Generalized T-stress Components under Uniform Loading Conditions

From the closed-form solutions presented in Sections 3.1–3.4, it is apparent that the value of the generalized T-stress components T_{13}, T_{14}, T_{34} is independent of the uniform crack-face, normal traction and uniform crack-face electrical charge, dependent only on the in-plane components of the remote triaxial stresses and remote electrical inductions, and independent of the electrical crack-face conditions. In addition, for the permeable case, the out-of-plane electrical induction d_3^∞ shows no contribution to both the mechanical T-stress components T_{11}, T_{33}, T_{13} and the electrical T-stress components T_{14}, T_{34}. By integrating the effect of the dielectric permittivity of a medium within the crack gap, both electrically semi-permeable and energetically consistent cases introduce a new parameter d_3^c which significantly influences the values of the generalized T-stress components T_{11} and T_{33}.

To demonstrate the effect of the crack-face conditions and the remote mechanical/electrical loading, the generalized T-stress components of a circular crack under the uniform remote triaxial stresses $2\sigma_{11}^\infty = \sigma_0$, $\sigma_{22}^\infty = \sigma_0$, $2\sigma_{33}^\infty = \sigma_0$ and the uniform remote electrical inductions $2d_1^\infty = d_0$, $d_2^\infty = d_0$, $2d_3^\infty = d_0$ are computed and reported in Figure 4-5 to Figure 4-12 for electrically impermeable, electrically permeable, electrically semi-permeable, and energetically consistent cracks. In the numerical study, the dielectric permittivity of a medium within the crack cavity for both electrically semi-permeable and energetically consistent cracks is taken to be $\varepsilon_c / \varepsilon_0 = 0.1$ where $\varepsilon_0 = 8.85 \times 10^{-12} \mathrm{C}/(\mathrm{Vm})$ is the value of the dielectric permittivity of the air. In addition, the normalized generalized T-stress components at $\theta = 0$ are also reported as a function of the normalized dielectric permittivity $\varepsilon_c / \varepsilon_0$ for the remote mechanical load and the combined remote mechanical/electrical loads in Figure 4-11 and Figure 4-12, respectively.

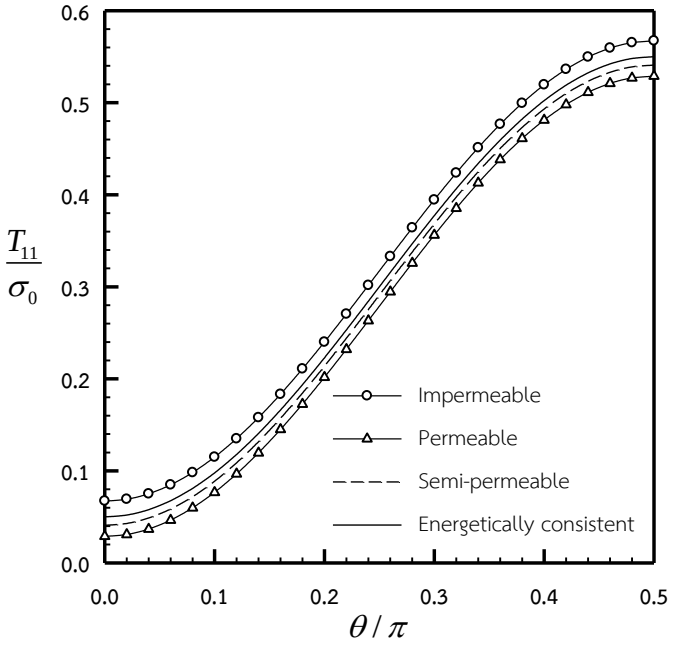

Figure 4-5: Normalized generalized T-stress component T_{11} along the crack front. Results are obtained for $\varepsilon_c/\varepsilon_0 = 0.1, \sigma_0 = 1\times10^6\,\text{Pa}$ and $d_0 = 0$.

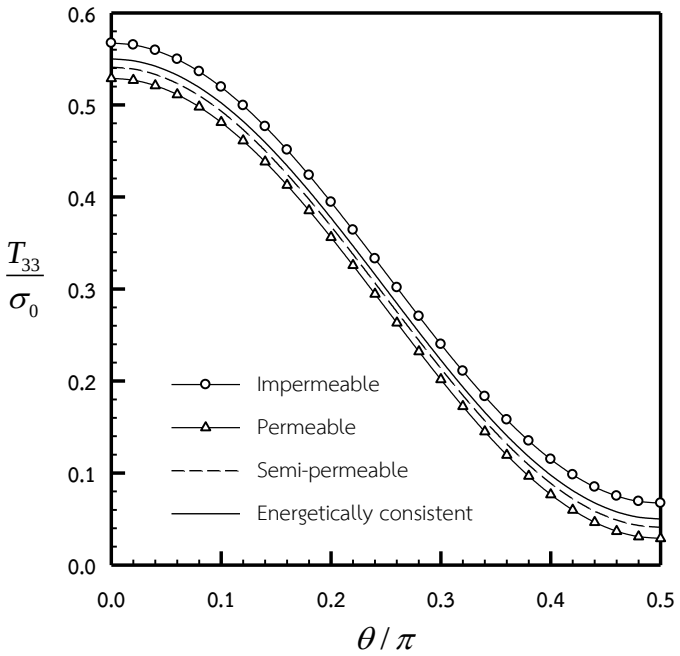

Figure 4-6: Normalized generalized T-stress component T_{33} on crack boundary. Results are obtained for $\varepsilon_c/\varepsilon_0 = 0.1, \sigma_0 = 1\times10^6\,\text{Pa}$ and $d_0 = 0$.

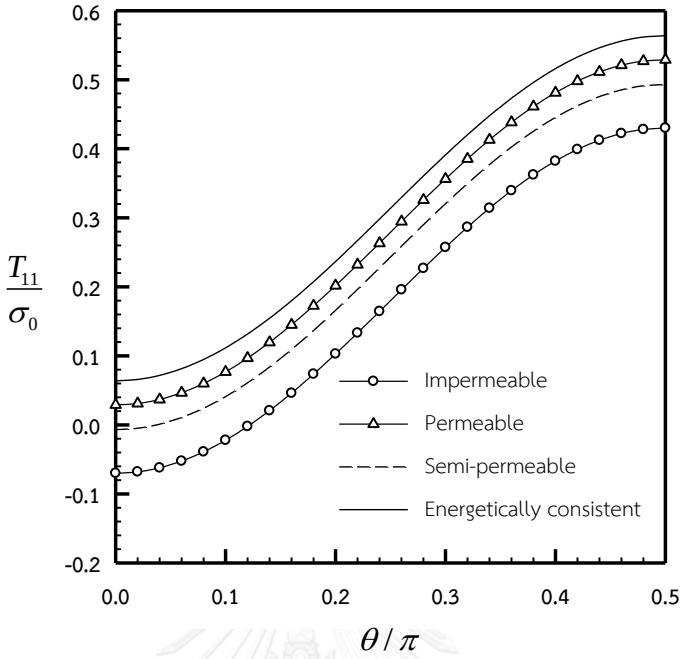

Figure 4-7: Normalized generalized T-stress component T_{11} on crack boundary. Results are obtained for $\varepsilon_c / \varepsilon_0 = 0.1, \sigma_0 = 1\times10^6 \text{Pa}$ and $d_0 = 1\times10^{-3}\text{C/m}^2$.

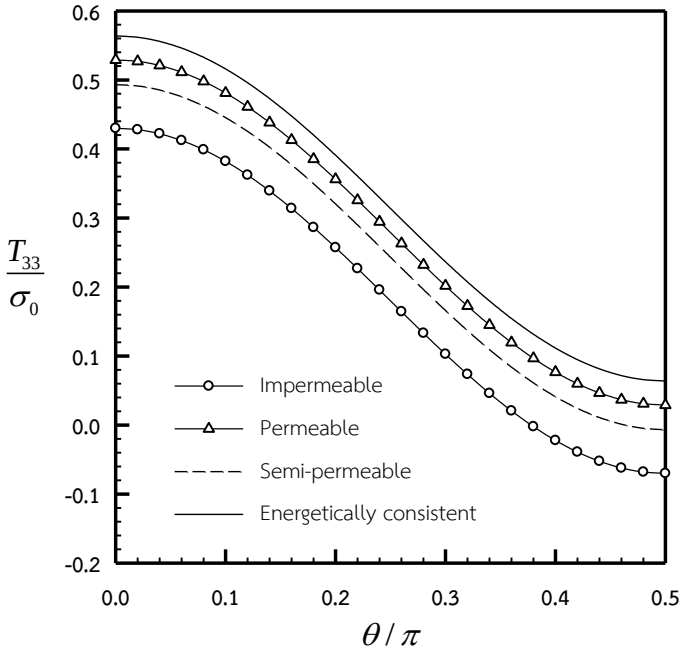

Figure 4-8: Normalized generalized T-stress component T_{33} along the crack front. Results are obtained for $\varepsilon_c / \varepsilon_0 = 0.1, \sigma_0 = 1\times10^6 \text{Pa}$ and $d_0 = 1\times10^{-3}\text{C/m}^2$.

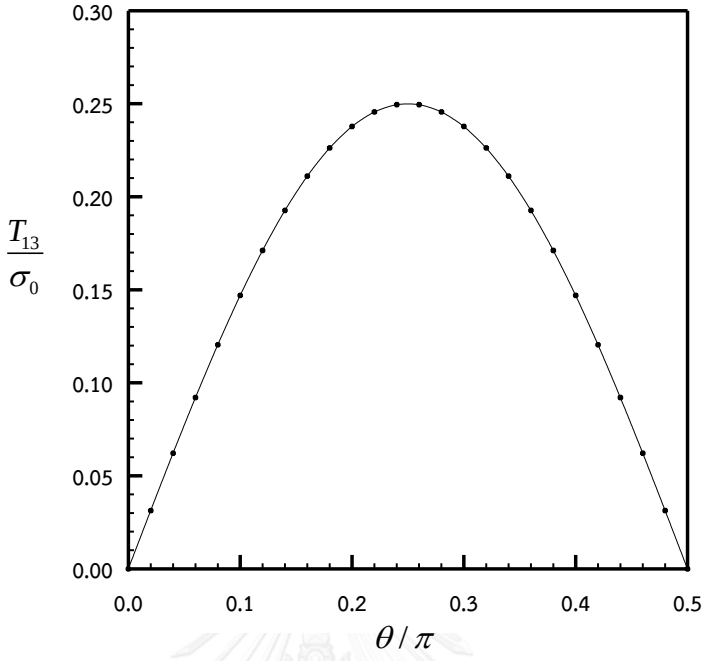

Figure 4-9: Normalized generalized T-stress component T_{13} along the crack front for all crack-face conditions and $\sigma_0 = 1\times10^6\,\mathrm{Pa}$

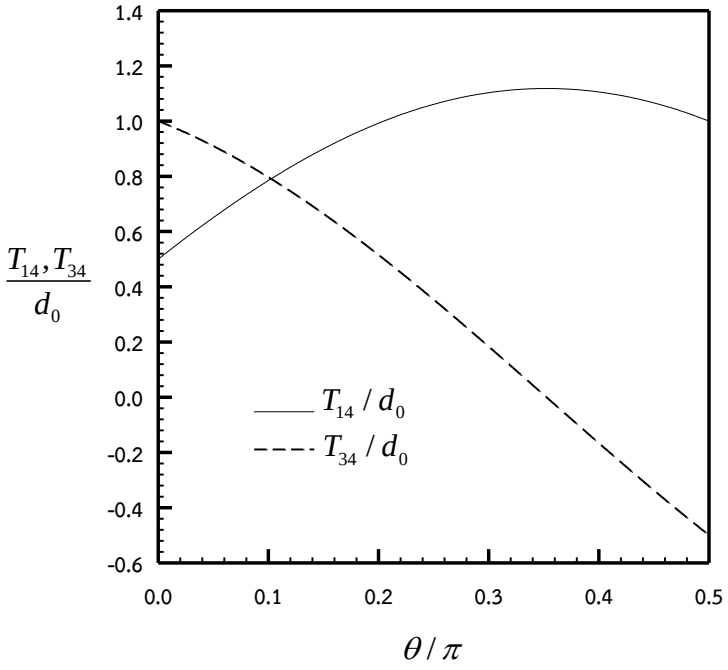

Figure 4-10: Normalized generalized T-stress components T_{14} and T_{34} along the crack front for all crack-face conditions and $\sigma_0 = 1\times10^6\,\mathrm{Pa}$ and $d_0 = 1\times10^{-3}\,\mathrm{C/m^2}$

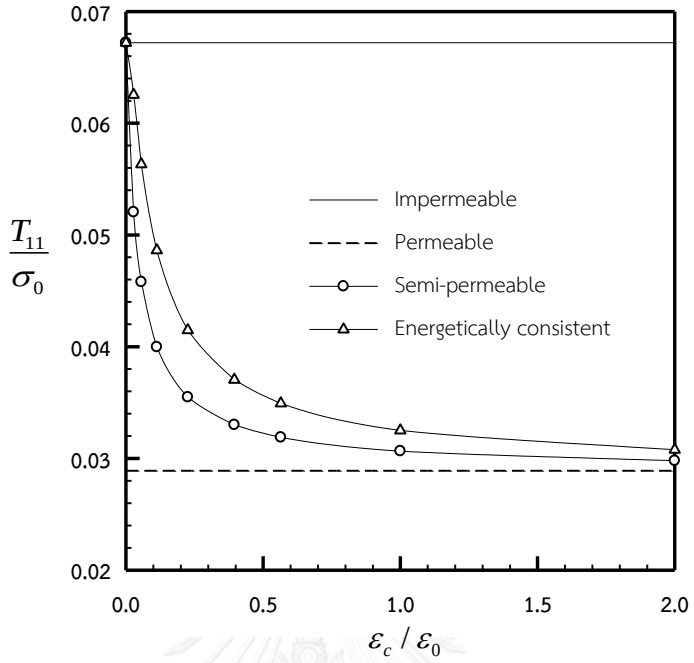

Figure 4-11: Normalized generalized T-stress component T_{11} at $\theta = 0$ versus the normalized dielectric permittivity $\varepsilon_c/\varepsilon_0$ for $\sigma_0 = 1\times10^6\,\mathrm{Pa}$ and $d_0 = 0$

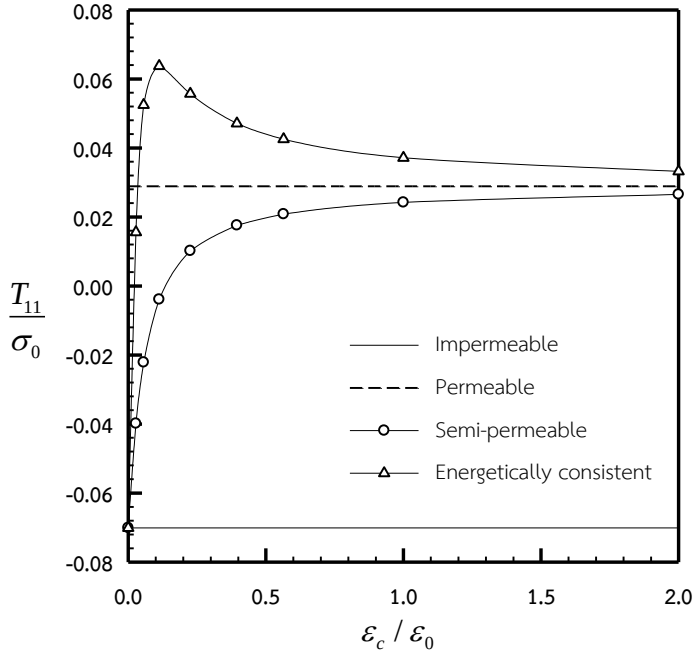

Figure 4-12: Normalized generalized T-stress component T_{11} at $\theta = 0$ versus the normalized dielectric permittivity $\varepsilon_c/\varepsilon_0$ for $\sigma_0 = 1\times10^6\,\mathrm{Pa}$ and $d_0 = 1\times10^{-3}\,\mathrm{C/m^2}$

It is evident from these results that for a medium subjected only to the remote triaxial stresses (i.e., $d_0 = 0$), the electrically impermeable and electrically permeable crack models yield, respectively, the upper and lower bound solutions of the generalized T-stress components T_{11} and T_{33} on the entire crack boundary (see Figure 4-5 and Figure 4-6). In addition, the generalized T-stress components T_{11}, T_{33} predicted by the semi-permeable model are only slightly different from the lower bound solution generated by the permeable case while solutions obtained from the energetically consistent crack model fall in between the electrically impermeable and permeable solutions. For this particular loading case, the generalized T-stress component T_{13} is independent of the crack-face conditions and its variation along the crack boundary due to the influence of the in-plane remote stresses is clearly indicated in Figure 4-9 whereas the components T_{14} and T_{34} identically vanish.

Unlike the previous case, for a combined remote mechanical/electrical loading (i.e., $\sigma_0 = 1\times10^6\,\mathrm{Pa}$ and $d_0 = 1\times10^{-3}\,\mathrm{C/m^2}$), the upper and lower bounds of the generalized T-stress components T_{11} and T_{33} change to those generated by the energetically consistent and impermeable models, respectively (see Figure 4-7 and Figure 4-8). It can be also seen from these results that T_{11} and T_{33} generated by the impermeable model are significantly different from solutions predicted by the other three crack-face models. In addition, T_{13} is still identical to the previous case whereas T_{14} and T_{34} are now non-zero but still independent of the crack-face conditions. The variation of T_{14} and T_{34} along the crack front is due mainly to the influence of the non-zero in-plane electric inductions d_1^∞, d_2^∞ as indicated in Figure 4-10.

To further demonstrate the influence of the dielectric permittivity of the medium within the crack cavity on the value of the generalized T-stress components, results are obtained for a range of $\varepsilon_c/\varepsilon_0$ from 0 to 2. Since the behavior of both components T_{11} and T_{33} is similar for the entire crack boundary as indicated above and T_{13}, T_{14}, T_{34} are independent of the crack-face conditions, it is sufficient to report only the generalized T-stress component T_{11} at a representative location at $\theta = 0$ along the crack-front as indicated in Figure 4-11 and Figure 4-12. In the absence of the remote electrical loading (see Figure 4-11), it is apparent that the electrically

permeable and impermeable solutions constitute the lower and upper bounds, respectively. In addition, as the dielectric permittivity increases from zero, semi-permeable and energetically consistent solutions start deviating from the impermeable solution and gradually converging to that of the permeable case for a sufficiently large value of $\varepsilon_c/\varepsilon_0$. For the case of combined remote triaxial stresses and electric inductions, the permeable and impermeable models yield the upper and lower bounds of the semi-permeable solution for the entire range of $\varepsilon_c/\varepsilon_0$ considered (see Figure 4-12). However, results of the energetically consistent case show that as the dielectric permittivity increases from zero, the value of T_{11} increases rapidly to its peak value above the permeable solution and then gradually decreases monotonically to that predicted by the permeable model.

4.3 Influence of Crack-face Mechanical Loading on Generalized T-stress

In this final section, the influence the distribution of the self-equilibrated, normal traction acting to the crack surface on the generalized T-stress components for both electrically permeable and impermeble cracks is studied.

Consider a circular crack under an axisymmetric, self-equilibrated, crack-face normal traction $t_3 = \sigma_0 \left(r/a \right)^n$ where σ_0 is a constant representing the maximum value of the traction along the crack front and n is an exponent indicating the distribution of traction across the crack surface. The resultant force of this traction can be readily computed and denoted by $T_0 = 2\pi\sigma_0 a^2/(n+2)$. It can be remarked that the exact solution of the generalized T-stress is available for the special case of $n=0$ in Section 3.1 and Section 3.2. For this particular problem, only the generalized T-stress components T_{11} and T_{33} are non-zero and are apparently independent of the position along the crack front for impermeable and permeable cases. The computed generalized T-stress components T_{11} and T_{33}, normalized either by the maximum value of the traction σ_0 or the resultant force T_0, are reported as a function of the exponent n in Figure 4-14 to Figure 4-17. As indicated by results in Figure 4-14 and Figure 4-15, the normalized generalized T-stress component T_{11} decreases monotonically in magnitude as the exponent n whereas the reverse effect is observed for the component T_{33} for both crack-face conditions.

Note also that both T_{11} and T_{33} are negative and, for a fixed value of the exponent n, the permeable model yields higher T_{11} and T_{33} in magnitude than those generated by the impermeable model. By changing the means of normalization (from σ_0 to $T_0 / \pi a^2$), it is clear from Figure 4-16 and Figure 4-17 that the normalized generalized T-stress T_{11} and T_{33} depends linearly on the exponent n. In particular, as n increases, the normalized T-stress components increase in magnitude.

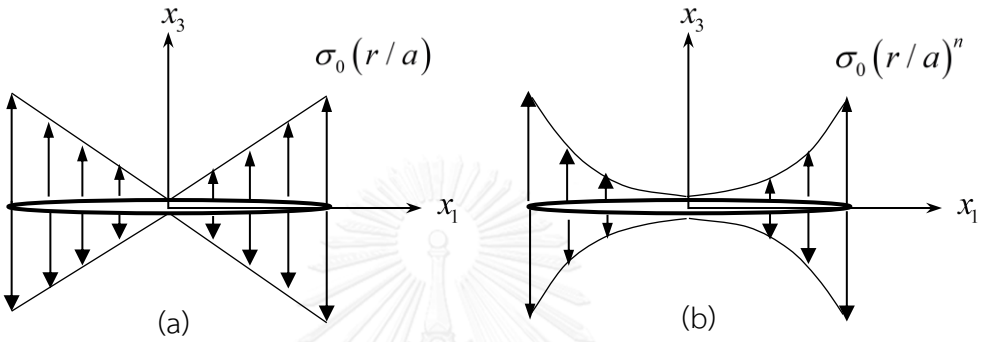

Figure 4-13: Circular crack under axisymmetric, self-equilibrated, crack-face, normal traction $\sigma_0 (r/a)^n$: (a) $n=1$ and (b) any generic value of n

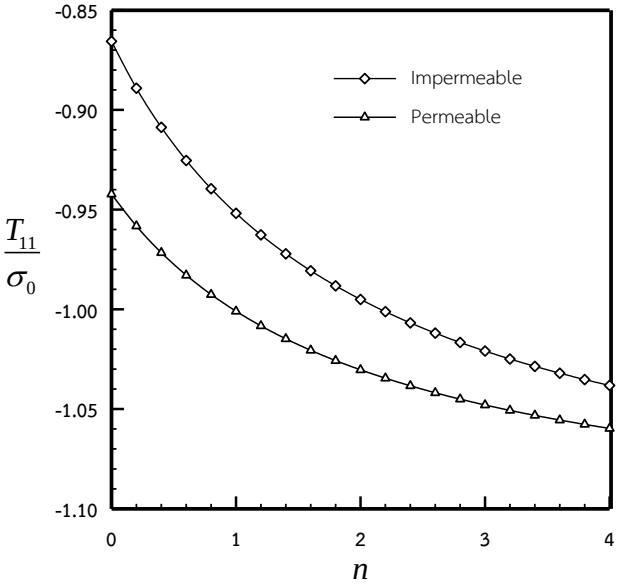

Figure 4-14: Normalized generalized T-stress components T_{11} of circular crack under axisymmetric, self-equilibrated, crack-face, normal traction $t_3 = \sigma_0 (r/a)^n$. Results are normalized by maximum value of traction σ_0.

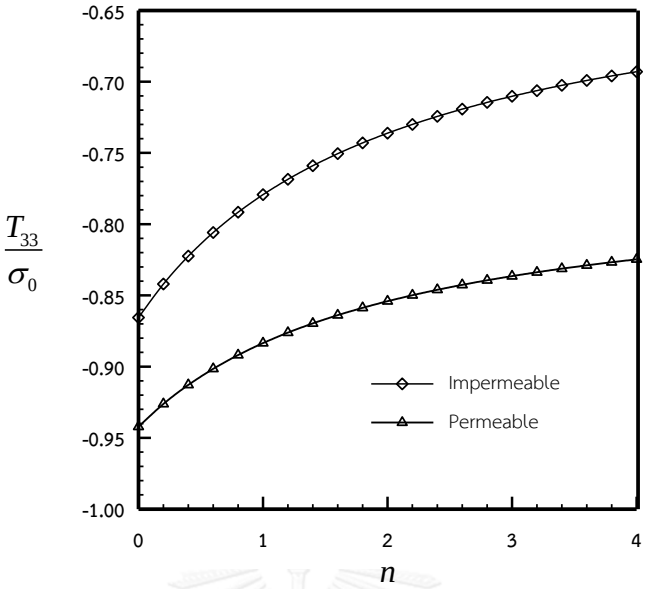

Figure 4-15: Normalized generalized T-stress components T_{33} of circular crack under axisymmetric, self-equilibrated, crack-face, normal traction $t_3 = \sigma_0 \left(r / a \right)^n$. Results are normalized by maximum value of traction σ_0.

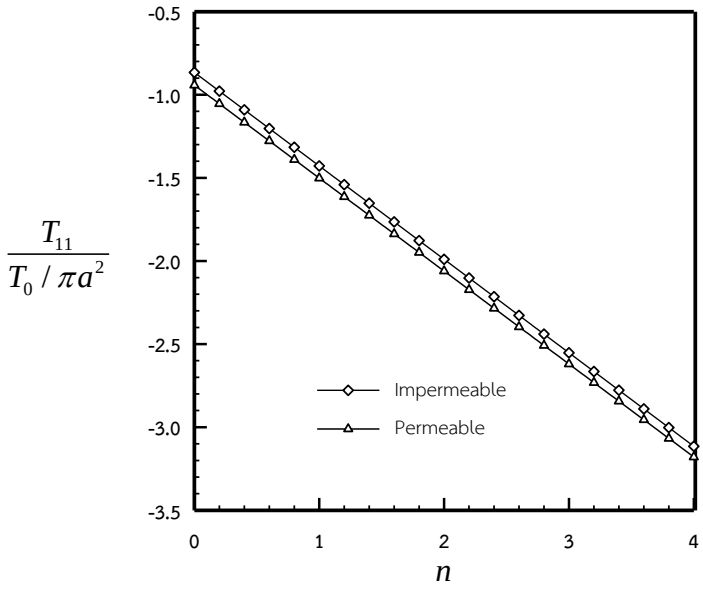

Figure 4-16: Normalized generalized T-stress components T_{11} of circular crack under axisymmetric, self-equilibrated, crack-face, normal traction $t_3 = \sigma_0 \left(r / a \right)^n$. Results are normalized by resultant force of traction T_0.

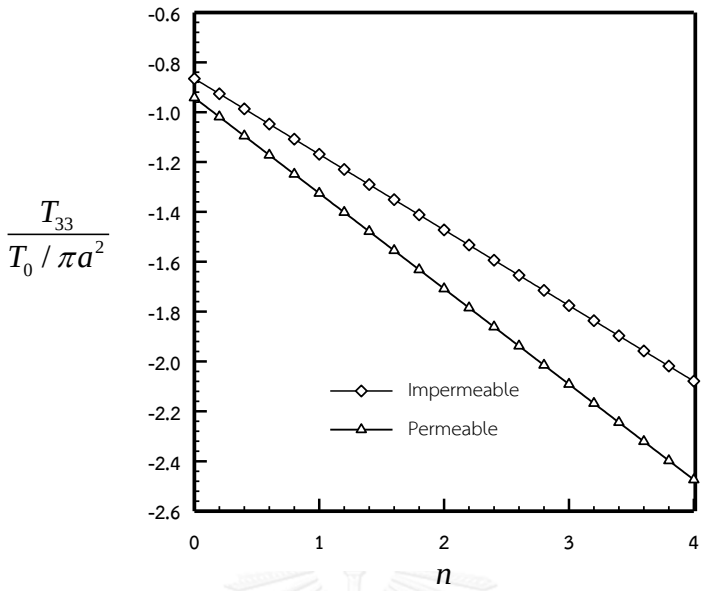

Figure 4-17: Normalized generalized T-stress components T_{33} of circular crack under axisymmetric, self-equilibrated, crack-face, normal traction $t_3 = \sigma_0 \left(r / a \right)^n$. Results are normalized by resultant force of traction T_0

Chapter 5

CONCLUSION

An exact solution of the generalized T-stress components for a circular crack contained in a three-dimensional, transversely isotropic, linear piezoelectric, infinite body under electrically permeable, im permeable, semi-permeable and energetically consistent crack-face conditions and subjected to both a uniform generalized far field and uniformly distributed crack-face mechanical/electrical loading has been derived. In addition, for both permeable and impermeable crack-face conditions, the generalized T-stress Green's function due to a pair of opposite, unit concentrated crack-face loads and the integral formula equipped with the numerical quadrature for calculating the generalized T-stress components under general loading conditions have been also established. In the derivation, existing generalized stress fields for various cases have been employed together with the near-front expansion and standard differentiations and proper limiting procedures. The obtained analytical solutions are explicit and involve only elementary functions, and they can be used as a basis for the parametric study to explore the effect of loading conditions, crack-face conditions and material properties on the generalized T-stress components along the crack boundary. In addition, the derived solutions can be also employed as the reliable benchmark solutions in the validation procedure of newly developed numerical schemes (e.g., boundary element and finite element methods) for analysis of general and complex crack problems.

The implemented integral formula using the proposed numerical quadrature has been also tested for several scenarios and it has been indicated that obtained results are in very good agreement with benchmark solutions. Additionally, results from a preliminary parametric study have shown that both the crack-face conditions and crack-face loading play an important role on the generalized T-stress along the crack boundary. To gain an in-depth understanding of the effect of many parameters on the generalized T-stress, a more extensive parametric study is still required and

solutions and formula obtained from the present study should provide a useful basis for such investigation.

REFERENCES

Ayatollahi, M., & Safari, H. (2003). Evaluation of crack tip constraint using photoelasticity. *International journal of pressure vessels and piping, 80*(9), 665-670.

Chen, W., & Lim, C. (2005). 3D point force solution for a permeable penny-shaped crack embedded in an infinite transversely isotropic piezoelectric medium. *International Journal of Fracture, 131*(3), 231-246.

Chen, W., & Shioya, T. (1999). Fundamental solution for a penny-shaped crack in apiezoelectric medium. *Journal of the Mechanics and Physics of Solids, 47*(7), 1459-1475.

Chen, W., Shioya, T., & Ding, H. (2000). A penny-shaped crack in piezoelectrics: resolved. *International journal of fracture, 105*(1), 49-56.

Chen, Y. (2000). Closed form solutions of T-stress in plane elasticity crack problems. *International journal of solids and structures, 37*(11), 1629-1637.

Cotterell, B., & Rice, J. (1980). Slightly curved or kinked cracks. *International Journal of Fracture, 16*(2), 155-169.

Du, Z.-Z., & Hancock, J. (1991). The effect of non-singular stresses on crack-tip constraint. *Journal of the Mechanics and Physics of Solids, 39*(4), 555-567.

Fabrikant, V. I. (1989). Application of Potential Theory in Mechanics. *Selection of New ResultsKluwer Academic, Dortrecht*.

Fett, T. (1997). A Green's function for T-stresses in an edge-cracked rectangular plate. *Engineering fracture mechanics, 57*(4), 365-373.

Fett, T. (1998). T-stresses in rectangular plates and circular disks. *Engineering fracture mechanics, 60*(5), 631-652.

Fett, T. (2001). Stress intensity factors and T-stress for internally cracked circular disks under various boundary conditions. *Engineering fracture mechanics, 68*(9), 1119-1136.

Fett, T. (2002). Stress intensity factors and T-stress for single and double-edge-cracked circular disks under mixed boundary conditions. *Engineering fracture mechanics, 69*(1), 69-83.

Fett, T., & Rizzi, G. (2006). T-stress of cracks loaded by near-tip tractions. *Engineering fracture mechanics, 73*(13), 1940-1946.

Fett, T., Rizzi, G., & Bahr, H.-A. (2006). Green's functions for the T-stress of small kink and fork cracks. *Engineering fracture mechanics, 73*(10), 1426-1435.

Hao, M., & Biao, W. (2004). T-stress in piezoelectric solid. *Applied Mathematics and Mechanics, 25*(5), 513-517.

Hao, T.-H., & Shen, Z.-Y. (1994). A new electric boundary condition of electric fracture mechanics and its applications. *Engineering fracture mechanics, 47*(6), 793-802.

Kirilyuk, V., & Levchuk, O. (2007). Elastic T-stress solutions for flat elliptical cracks under tension and bending. *Engineering fracture mechanics, 74*(17), 2881-2891.

Landis, C. M. (2004). Energetically consistent boundary conditions for electromechanical fracture. *International journal of solids and structures, 41*(22), 6291-6315.

Larsson, S.-G., & Carlsson, A. J. (1973). Influence of non-singular stress terms and specimen geometry on small-scale yielding at crack tips in elastic-plastic materials. *Journal of the Mechanics and Physics of Solids, 21*(4), 263-277.

Li, Q., Ricoeur, A., & Kuna, M. (2011). Coulomb traction on a penny-shaped crack in a three dimensional piezoelectric body. *Archive of Applied Mechanics, 81*(6), 685-700.

Li, X.-F., & Lee, K. Y. (2004a). Crack growth in a piezoelectric material with a Griffith crack perpendicular to the poling axis. *Philosophical Magazine, 84*(18), 1789-1820.

Li, X.-F., & Lee, K. Y. (2004b). Three-dimensional electroelastic analysis of a piezoelectric material with a penny-shaped dielectric crack. *Journal of applied mechanics, 71*(6), 866-878.

Limwibul, V., Jaroon Rungamornat, & Phongtinnaboot, W. (2016). *Analysis for Generalized T-stresses of Cracks in 3D Piezoelectric Media under Various Crack-Face Conditions*. Paper presented at the 21st National Convention on Civil Engineering, Songkhla, Thailand.

Liu, S., Shen, Y., & Liu, J. (2012). Exact solutions for piezoelectric materials with an elliptic hole or a crack under uniform internal pressure. *Chinese Journal of Mechanical Engineering, 25*(4), 845-852.

Matvienko, Y. G. (2014). The Effect of the non-singular T-stress components on crack tip plastic zone under mode I loading. *Procedia Materials Science, 3*, 141-146.

Matvienko, Y. G., & Pochinkov, R. (2013). Effect of nonsingular T-stress components on the plastic-deformation zones near the tip of a mode I crack. *Russian Metallurgy (Metally), 2013*(4), 262-271.

McMeeking, R. M. (2004). The energy release rate for a Griffith crack in a piezoelectric material. *Engineering fracture mechanics, 71*(7), 1149-1163.

Parton, V. Z. (1976). Fracture mechanics of piezoelectric materials. *Acta Astronautica, 3*(9), 671-683.

Qu, J., & Wang, X. (2006). Solutions of T-stresses for quarter-elliptical corner cracks in finite thickness plates subject to tension and bending. *International journal of pressure vessels and piping, 83*(8), 593-606.

Rungamornrat, J., & Mear, M. E. (2008). Analysis of fractures in 3D piezoelectric media by a weakly singular integral equation method. *International Journal of Fracture, 151*(1), 1-27.

Rungamornrat, J., Phongtinnaboot, W., & Wijeyewickrema, A. (2015). Analysis of cracks in 3D piezoelectric media with various electrical boundary conditions. *International journal of fracture, 192*(2), 133-153.

Rungamornrat, J., & Pinitpanich, M. (2016). T-stress solution of penny-shaped cracks in transversely isotropic elastic media. *Engineering Fracture Mechanics, 158*, 194-208.

Shahani, A., & Tabatabaei, S. (2009). Effect of T-stress on the fracture of a four point bend specimen. *Materials & Design, 30*(7), 2630-2635.

Sladek, J., & Sladek, V. (1997). Evaluations of the T-stress for interface cracks by the boundary element method. *Engineering fracture mechanics, 56*(6), 813-825.

Subsathaphol, T. (2013). *Analysis of T-stress for cracks in 3D linear piezoelectric media.* (Master degree), Chulalongkorn University.

Viola, E., Boldrini, C., & Tornabene, F. (2008). Non-singular term effect on the fracture quantities of a crack in a piezoelectric medium. *Engineering Fracture Mechanics, 75*(15), 4542-4567.

Wang, X. (2002). Elastic T-stress for cracks in test specimens subjected to non-uniform stress distributions. *Engineering fracture mechanics, 69*(12), 1339-1352.

Wang, X. (2003). Elastic T-stress solutions for semi-elliptical surface cracks in finite thickness plates. *Engineering fracture mechanics, 70*(6), 731-756.

Wang, X. (2004). Elastic T-stress solutions for penny-shaped cracks under tension and bending. *Engineering fracture mechanics, 71*(16), 2283-2298.

Wang, X., & Bell, R. (2004). Elastic T-stress solutions for semi-elliptical surface cracks in finite thickness plates subject to non-uniform stress distributions. *Engineering fracture mechanics, 71*(9), 1477-1496.

Williams, M. L. (1957). On the stress distribution at the base of a stationary crack. *ASME Journal of Applied mechanics, 24*, 109-114.

Yang, B., & Ravi, C. K. (1999). Evaluation of elastic T-stress by the stress difference method. *Engineering fracture mechanics, 64*(5), 589-605.

Zhao, L., Tong, J., & Byrne, J. (2001). Stress intensity factor K and the elastic T-stress for corner cracks. *International Journal of Fracture, 109*(2), 209-225.

Zhong, X.-C., & Li, X.-F. (2008). T-stress analysis for a Griffith crack in a magnetoelectroelastic solid. *Archive of Applied Mechanics, 78*(2), 117-125.

Zhou, C., & Li, Z. (2007). The effect of T-stress on crack–inclusion interaction under mode I loading. *Mechanics Research Communications, 34*(3), 283-288.

Zhou, R., Zhu, P., & Li, Z. (2011). The shielding effect of the plastic zone at mode-II crack tip. *International Journal of Fracture, 171*(2), 195-200.

Zhou, Z., Xu, X., Leung, A. Y., & Huang, Y. (2013). Stress intensity factors and T-stress for an edge interface crack by symplectic expansion. *Engineering fracture mechanics, 102*, 334-347.

Zhu, T., & Yang, W. (1999). Crack kinking in a piezoelectric solid. *International journal of solids and structures, 36*(33), 5013-5027.

APPENDIX

VITA

Mr. Vichet Chan Pich was born on October 30, 1991. After graduating bachelor degree from Institute of Technology of Cambodia (ITC) in 2014, he obtained scholarship from JICA to continue his Master degree in major Structural Engineering in Chulalongkorn University in Thailand. Finally, after a year of study in Civil Engineering, he began to conduct his research in field of Solid Mechanic under supervision of Assoc. Prof. Dr. Ajarn Rungamornrat and Dr. Weeraporn Phongtinnaboot.